The Rotating Solar Boiler

Master Thesis
By
Jeroen van Luijtelaer, BSc.

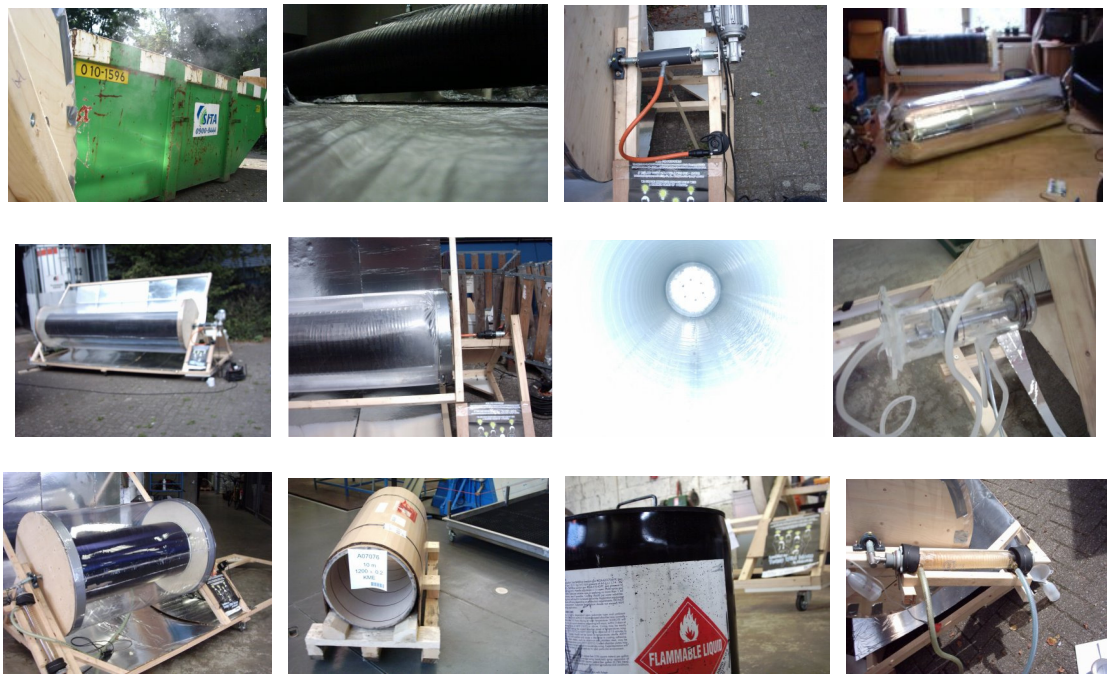

Supervisor:
Prof. Dr. Geert-Jan Witkamp

March 31, 2006

The Rotating Solar Boiler

Master Thesis
By

Jeroen van Luijtelaer, BSc.

Name:	J. P. H. van Luijtelaer, BSc.
E- mail:	J.P.H.vanLuijtelaer@tudelft.nl
Study:	Chemical Engineering
	Delft University of Technology
Date:	March 31, 2006
Supervisors:	Prof. Dr. G. J. Witkamp
	Ir. A. Schmets
	Drs. J. van Spronsen

Preface

Today (February 4th, 2005) the rotating solar boiler produced steam for the first time. Although it is mid winter and 10°C and the air looked moist and white the sun provided enough energy to attain the design temperature of 100°C. The prototype costs less than 100 euro for materials and has an effective area of about 1 m^2. I am pleased with how the practical work confirms the theoretical work and I am convinced the work can be pushed towards commercialization.

Summary

Rotating solar boilers are a new type of solar collector. The boilers consist of two concentric tubes. The inner tube absorbs sunlight and boils water. This tube is called the absorber. The outer transparent tube is filled with air and called the cover. The boilers rotate at 60 rpm to completely prevent convection in the insulating air layer in between the tubes.

Three prototypes were built using different materials of construction. Absorbers made of painted galvanized steel and sputtered copper were evaluated experimentally. The sputtered coating proved to be superior to the paint.

The boilers typically produced 1 kW of steam at 100^{o}C. The efficiencies of the different boilers were measured. A model was developed to predict their performance. The model predicts an efficiency of 68%. For the most advanced prototype the maximum experimental efficiency with reflectors was 46%. The discrepancy between these values may be due to fouling of the selective surface, misalignment of the reflectors or the error in measurement of steam production.

This prototype was fitted with a clean absorber and measurements without reflectors were taken. The model then predicts an efficiency of 62%. An experimental efficiency of 61% was measured.

Economical analyses were performed as well. These analyses showed that any solar boiler should be very lightweight in order to reduce material cost. The rotating solar boiler can be lighter and cheaper than conventional flat plate collectors and evacuated tube collectors.

In the chapter on future work a completely inflatable rotating solar boiler is proposed. This boiler can have a pay back time of less than 1 year.

Table of contents

Table of contents

1. Introduction

Solar collectors are devices that produce heat from the sun. Currently they are the most economic means of converting solar energy into useable energy. The heat generated by solar collectors can be used for pool heating, domestic hot water supply, distilling saline water and many other purposes. Furthermore, if the operation temperature is sufficient, electric power generation can be feasible. The thermoelectric conversion can compete with photovoltaic electricity generation.
A lot of research has been put into the development of efficient collectors. A successful solar collector has a high efficiency, produces high temperatures and has a low cost per surface area. The maximum cost per surface area should be below 152 €/m^2. This number can be calculated using a yearly average solar irradiation of 2.67 $kWh \cdot day^{-1} \cdot m^{-2}$ (ref. 1), and a gas price of 0.052 €/kWh (ref. 2). The amount of money that can be saved per year is thus $2.67 \cdot 365 \cdot 0.052 = 50.68$ $€ \cdot m^{-2}$.If an efficiency of 60% is assumed and a pay back time of 5 years is desired the maximum price for a solar collector becomes $50.68 \cdot 0.60 \cdot 5 =$ 152 €/m^2. If the collector is much more expensive it will never repay itself. If the collector is less expensive the interest rate and the collector efficiency determine the economic feasibility. This maximum price severely limits the design options and contemporary high temperature solar collectors do not meet this demand. Low temperature solar collectors can meet this demand, but the market for low temperature heat is small (ref. 3).
Solar boilers can reduce CO_2 emissions considerably (ref. 4), and have the potential to reduce the greenhouse effect. Therefore, a design for a cheap high temperature solar boiler is highly desired. In this thesis a new design is proposed and evaluated both theoretically and experimentally. The hypothesis is that in the new design a centrifugal force may prevent convective heat loss and this effect can be utilized to produce a cheaper and more efficient solar boiler.
In order to test the hypothesis a research approach was formulated. The existing methods for solar heat generation were studied. These solar collectors are described in the introduction and their advantages and disadvantages are mentioned. In the second chapter the rotating boiler terminology is explained and the theory behind the rotating solar boiler is elaborated. This theory is combined in a predictive model. In the third chapter iterative research is done. Three boilers were built. Each time a boiler was tested the results and conclusions were used in the following prototype.

The research goals are:

1. *Select suitable materials for the boiler*
2. *Develop a model in order to predict the performance of rotating solar boilers*
3. *Evaluate the efficiency of the solar boiler*
4. *Economic evaluation*

1. Introduction

At this moment there are five different types of solar collectors:

- Concentrating solar collectors
- Flat plate solar collectors
- Evacuated tube collectors
- Uncovered absorbers
- Solar ponds

These different types of conventional solar collectors will be described in the next paragraphs.

1.1 Concentrating solar collectors

This type of solar collector consists of parabolic mirrors that concentrate the light onto a spot or a line, where the heat is generated. The parabolic mirrors work like a magnifying glass. These collectors are efficient and can be produce energy at a very high temperature 300-500^{o}C). The reflectors should be made with sufficient precision in order to concentrate the rays of the sun onto a small area. Furthermore, tracking of the sun is necessary. This means that the collector is pointed towards the sun. The structure should be able to withstand wind. These collectors only perform well if the reflectors are clean and clouds do not obstruct the sun. The precision required makes the price per square meter high.

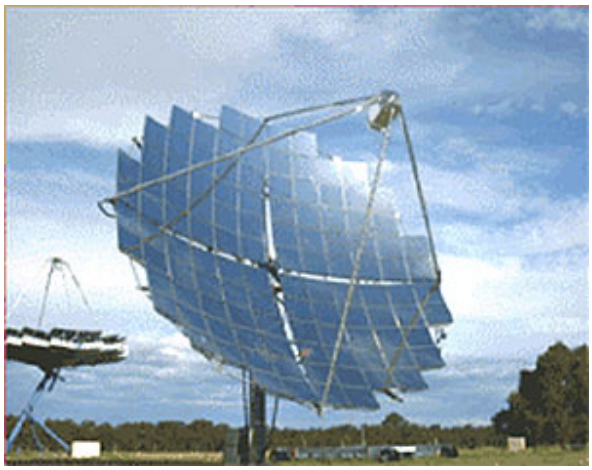

Figure 1.1: Concentrating solar collector (ref. 5)

1.2 Flat plate solar collectors

These collectors are generally used for water heating at moderate temperatures. They consist of a cover made of glass or plastic and an absorber plate with attached water tubes to heat up water. The sides and the bottom of the collector are insulated.

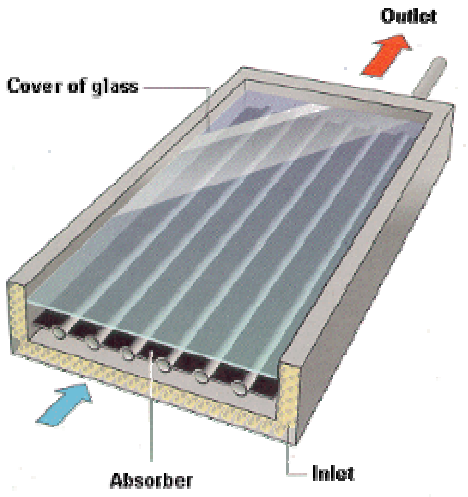

Figure 1.2: Flat plate solar collector (ref. 6)

Because the collector does not have to track the sun, it is relatively cheap. The efficiency is good at low temperatures but the large surface area leads to high heat losses at higher temperatures. Especially the heat loss due to convection between the absorber and the cover is substantial.

1.3 Evacuated tube collectors

The evacuated tube collector is a non-tracking solar collector. It consists of two concentric tubes made of borosilicate glass. It utilizes a vacuum between the tubes in order to eliminate conductive and convective losses. Generally they perform very well even in cold and overcast weather. The vacuum of less than 1 mPa is hard to maintain, and the glass needs to be quite thick in order to withstand both the weather conditions and the vacuum. These types of collectors are heavy and expensive. These collectors can be used at higher temperatures than flat plate collectors. Temperatures of over 100^{o}C are attainable.

Figure 1.3: Evacuated tube solar collector (ref. 7)

Evacuated collectors usually have reflectors to utilize the complete surface area of a round tube. These reflectors are static and do not have to be pointed at the sun. They do not concentrate but bend the light to suit the cylindrical geometry of the vacuum tube as can be seen in figure 1.4.

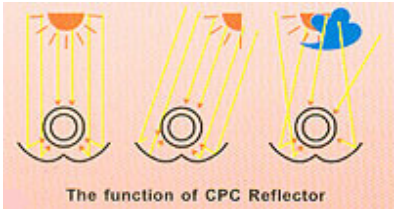

Figure 1.4: Reflectors for evacuated tube solar collectors (ref. 8)

This is the kind of collector that is most closely related to the rotating collector. The rotating boiler is compared with this type of collectors throughout this thesis.

1.4 Uncovered absorbers

Uncovered absorbers are black surfaces with incorporated water tubes. They have no additional means of retaining heat (figure 1.5). They are able to yield high efficiencies near ambient temperature (20-40^{0}C). The costs are very low, so the pay-back time is short. These absorbers are economical for pool heating, for domestic warm water supply in warm countries and may be used in combination with a heat pump. The efficiency drops very sharp at elevated operation temperatures. The market for low temperature heat is small because warm water (20-40^{o}C) has a limited number of applications.

Figure 1.5: Uncovered absorber by Hot Sun industries (ref. 9)

1.5 Solar ponds

A solar pond is a basin of water where convection is prevented. Water is used as an insulator and as a heat radiation barrier. Convection is prevented by a salt gradient or by layers of transparent plastic film. The solar pond has the advantage that it also stores the heat. Drawbacks are that the pond cannot be tilted towards the sun, and maintenance problems are abundant. This collector shows that preventing convection is an important step towards higher efficiency in solar collectors.

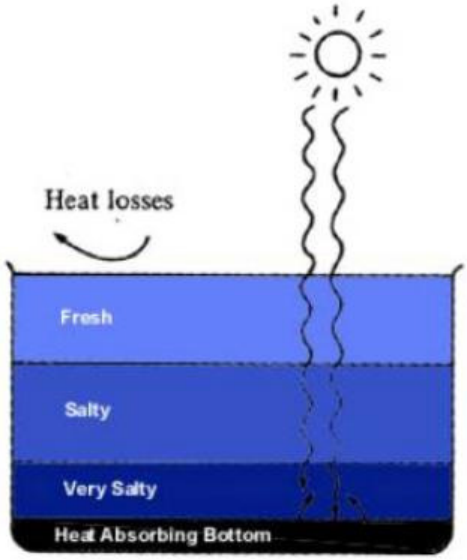

Figure 1.6: Schematics of a solar pond (ref. 10)

2. Rotating solar boiler theory

In this chapter the theory behind the rotating solar boiler is elaborated. In the first paragraph the terminology for the rotating solar boiler is explained. The following paragraphs give a description of the physical phenomena occurring in solar boilers. The effects of conduction, convection, radiation and mechanical losses are described. The phenomena that affect the rotating boiler's efficiency are included in the theoretical model that has been developed. In paragraph 2.6 the model is evaluated and compared to other solar collectors.

2.1 Terminology

The preliminary patent search indicated that the design is indeed new (see appendix 1). Therefore it is important to first explain some terms and give some definitions. The terms boiler and collector are both used for the same apparatus in this thesis. Now the individual parts of the rotating solar boiler are explained.

Figure 2.1: Absorber in its frame

1. Absorber also called absorber tube
2. Bearing
3. Axle

In figure 2.1 the absorber can be seen in its frame. The absorber is coated with a spectrally selective coating. This coating is also referred to as selective coating. There are two axles on the ends of the absorber. These axles are used to support the absorber and to transport the fluids to and from the absorber tube.

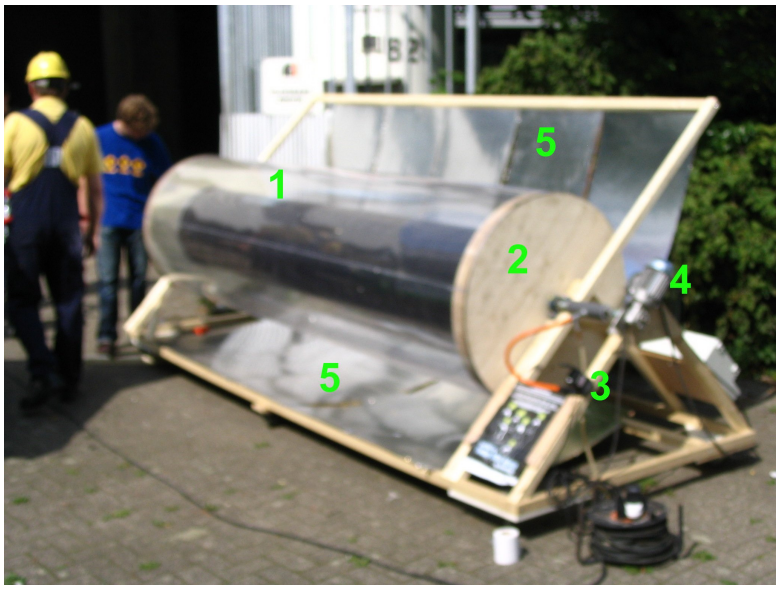

Figure 2.2: Completed solar boiler

1. Cover
2. End cap also called side
3. Air pump
4. Motor
5. Reflectors also called mirrors

The absorber is surrounded by the cover. The cover is made from transparent plastic. The empty space created between the absorber and the cover is called the air layer. The cover is inflated in order to make it retain its shape. This is done using the air pump.
The end caps are used to support the cover and insulate the absorber tube. They are made of polyurethane foam. The motor is used to rotate the boiler and the reflectors are used to maximize the light incident on the absorber. Three working rotating solar collectors where constructed. They are referred to as prototype 1, 2 and 3. (Figures 2.3-2.5)

Figure 2.3: Prototype 1

Prototype 1 was made in spare time and with own finances. The absorber was 1.0 m long and the diameter was 0.30 m. The most important conclusions from this prototype were that little energy is required to obtain sufficient rotation (8 Watt), and that the rotation prevents convection. The boiler was lost in a storm.

Figure 2.4: Prototype 2

The absorber of prototype 2 was 3.0 m long and 0.50 m diameter. It yielded 931 Watt of steam and had an efficiency of 25%. The selective surface was Solkote^{tm} HI/Sorb^{tm}-II paint from Solec^{tm}. There were too many unknown parameters to conclude that this boiler's performance was not predicted by the model.

Figure 2.5: Prototype 3

Prototype 3 measured 1.2 m length and 0.50 m diameter, for the absorber. The efficiency was 46% and the boiler delivered 0.8 kW of steam. The absorber is a copper tube with a wall thickness of 0.20mm and a high performance sputtered coating. The copper for the absorber was provided by Alanod Sunselect.

2.2 Conduction theory

One heat transfer effect that occurs in solar collectors is conduction. Heat conduction occurs due to thermal motion in molecules. Conduction gives rise to heat loss both through the air layer and through the sides of the boiler.

For flat layers like the end caps conductivity is linear with temperature difference according to:

$$\Phi_e^{cond} = \frac{\lambda_e}{d_e} \cdot A_e \cdot \Delta T \quad \text{(Eq. 2.1)}$$

with:

Φ_e^{cond}	Heat loss due to conduction through the end caps	[W]
λ_e	Heat transfer coefficient of end caps	[W/(m·K)]
d_e	Thickness of the end cap	[m]
A_e	Area of the end caps	[m^2]
ΔT	Temperature difference	[K]

Formula 2.1 is used to calculate the conductive losses through the end caps. In order to calculate the conductive heat loss through the air layer the equation is reworked to conduction through a tube:

$$\Phi_c^{cond} = \frac{2 \cdot l \cdot \lambda_{air} \cdot \pi \cdot \Delta T}{\ln\left(\frac{R_c}{R_a}\right)} \quad \text{(Eq. 2.2)}$$

with:

Φ_c^{cond}	Heat loss due to conduction through the cover	[W]
l	Length of the absorber	[m]
λ_{air}	Heat transfer coefficient of the air	[W/(m·K)]
R_a	Radius of the absorber	[m]
R_c	Radius of the cover	[m]

The conduction is very small if the radius of the cover is much larger than the radius of the absorber.

2.3 Convection theory

Natural convection is the movement of a fluid due to a difference in buoyancy.

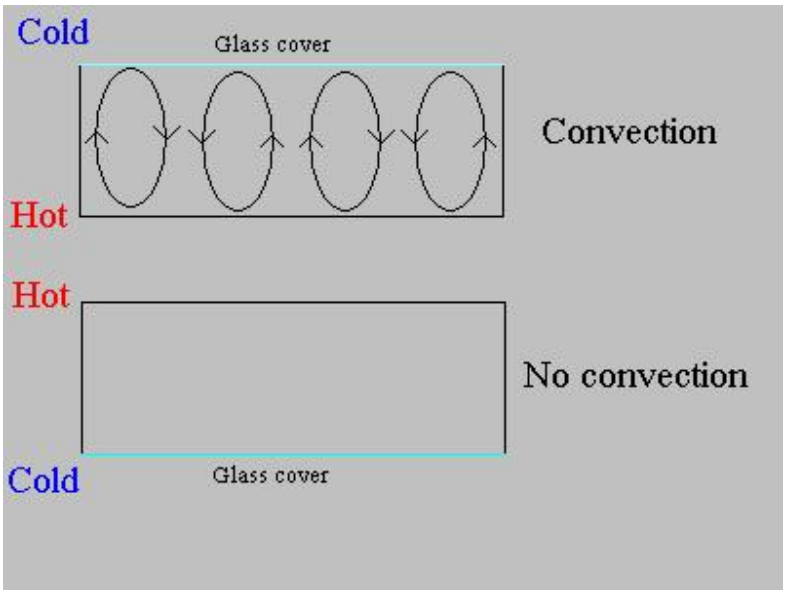

Figure 2.6: gravitation causes convection

Hot air is less dense than cold air and rises due to gravity. The hot air near the absorber of a flat plate collector is lighter than the colder air near the glass cover and hence it tends to rise towards the glass. There it cools down and sinks to the absorber plate. This effect cools down the absorber plate because air transports the heat from the absorber to the glass as can be seen in figure 2.6.
Convective losses can be estimated using the Nusselt number. The Nusselt number is the heat loss due to convection plus conduction divided by the conductive heat loss:

$$Nu = \frac{\Phi^{conv} + \Phi^{cond}}{\Phi^{cond}} \qquad \text{(Eq. 2.3)}$$

with:

Φ^{conv}	Convective heat loss	[W]
Nu	Nusselt number	[-]

If the Nusselt number is unity there is no convection. The Nusselt number can be estimated using the Grashof number multiplied by the Prandtl number ($Gr \cdot Pr$). Three regimes can be distinguished: (1) turbulent (2) laminar and (3) no convection (ref. 11):

$Nu = 1$ (No convection if $Gr \cdot Pr < 1800$)

$Nu = 0.15(Gr \cdot Pr)^{1/4}$ (Laminar convection if $10^4 < Gr \cdot Pr < 10^7$)

$Nu = 0.17(Gr \cdot Pr)^{1/3}$ (Turbulent convection if $Gr \cdot Pr > 10^7$)

where:

$$Gr \cdot Pr = \frac{d^3 \cdot g \cdot \Delta T}{\nu \cdot \overline{T} \cdot a} \qquad \text{(Eq. 2.4)}$$

with

$$a = \frac{\lambda}{\rho \cdot Cp} \qquad \text{(Eq. 2.5)}$$

and:

d	The thickness of the air layer	[m]
g	The gravitational constant	[ms^{-2}]
ΔT	The temperature difference	[K]
ν	Kinematic viscosity	[m^2s^{-1}]
$\overline{T}$	Average temperature	[K]
a	Heat diffusion coefficient	[m^2s^{-1}]
ρ	Density	[$kg \cdot m^{-3}$]
Cp	Heat capacity	[$J \cdot kg^{-1}K^{-1}$]

Formula 2.4 applies to ideal gasses. Atmospheric air in solar boilers behaves as an ideal gas so the formula is appropriate.

Placing the solar collector upside down prevents convection, because the direction of the gravitational field changes, yielding a negative $Gr \cdot Pr$. Adding a centrifugal force may also yield a negative $Gr \cdot Pr$ and thus eliminate convection. This is elaborated in the next paragraph.

2.3.1 Rotating the collector

Convection occurs due to gravity. Adding the centrifugal force to the system can have a dramatic effect. In a centrifuge denser material is pushed outwards. This also applies to air. In a centrifuge the colder (denser) air accumulates on the outside and the hotter (lighter) air is pushed inwards. This can be seen in figure 2.7:

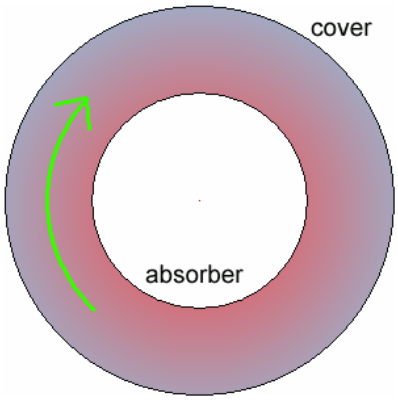

Figure 2.7: centrifugal acceleration prevents convection

The air between the cover and the absorber rotates with the same rotational speed as the cover and the absorber. This causes a centrifugal acceleration to act on the air layer. A modest rotation speed can already achieve this desired effect. The effect prevents convection completely when the centrifugal acceleration is greater than the gravitational acceleration:

$$\frac{v_a^2}{R_a} > g \qquad \text{(Eq. 2.6)}$$

with:

v_a velocity of the absorber [m/s]

If the absorber has a radius of 0.25 m (for prototype 2 and 3) the velocity becomes 1.6 m/s. This equals a rotation speed of $1.6/(2 \cdot \pi \cdot 0.25) \cdot 60 = 60$ RPM.

2.4 Radiation theory

Radiation is an important heat transport phenomenon in solar collectors. The collector is heated by the solar radiation. Furthermore any heated surface will also give off some radiation. This radiation is called thermal radiation. This radiation is infrared radiation. In order to predict the efficiency of any solar boiler the radiation effects of the absorber, the cover and the reflectors should be taken into account.

2.4.1 Heat radiation

The power lost by thermal radiation for the absorber is given by:

$$\Phi^{rad} = A_a \cdot \sigma \cdot \varepsilon_a \cdot \left(T_a^4 - T_c^4\right) \quad \text{(Eq 2.7)}$$

with:

Φ^{rad}	Radiative loss from the absorber	[W]
A_a	Area of the absorber	[m^2]
σ	Stefan-Boltzmann constant	[$Wm^{-2}K^{-4}$]
ε_a	Emission coefficient of the absorber	[-]
T_a	Absorber temperature	[K]
T_c	Cover temperature	[K]

The emission coefficient (also called emissivity or emittance) is the fraction of the total blackbody infrared radiation that is emitted. The Stefan-Boltzmann coefficient has a value of $5.67*10^{-8}$ $Wm^{-2}K^{-4}$. The wavelength distribution can be calculated using Planck's law (figure 2.8):

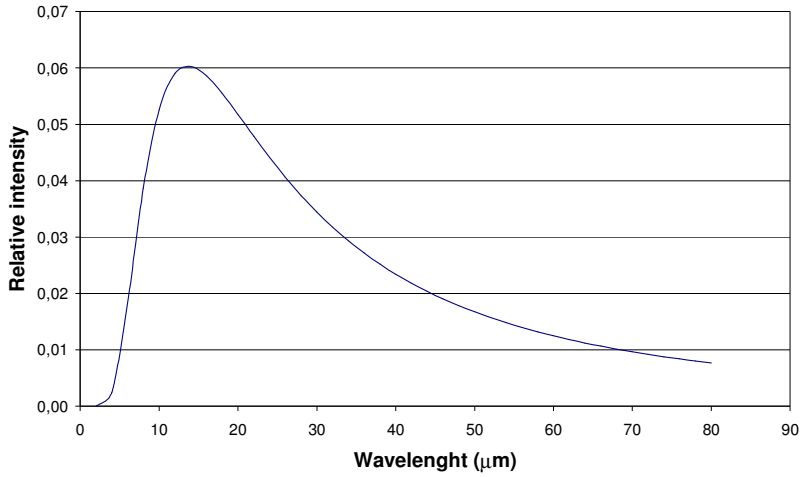

Figure 2.8: Relative intensity of blackbody radiation at T = 373 K as a function of the wavelength

The normalized curve shows that most of the heat radiation occurs at wavelengths larger than 10 μm.

2.4.2 Solar radiation

The solar radiation that is gained is given by:

$$\Phi^{in} = A_i \cdot \sigma \cdot \alpha_a \cdot \left(T_s^4 - T_a^4\right) \quad \text{(Eq 2.8)}$$

where:

$$A_i = 2 \cdot R_a \cdot l \quad \text{(Eq. 2.9)}$$

with:

Φ^{in}	Energy gained	[W]
T_s	Effective solar temperature	[K]
α_a	Absorption coefficient of the absorber	[-]
T_a	Absorber temperature	[K]
A_i	Illuminated absorber area	[m^2]
l	Length of the absorber tube	[m]

Formula 2.8 suggests that the solar energy that is gained is constant because the absorber temperature is much lower than the effective solar temperature. This however is not true. The solar energy that can be gained is dependent on the latitude, the attenuation of the atmosphere (clouds, etc) and the time of the day. Therefore the usual approach in solar energy research is to measure the influx of power that can be gained directly. This is called the insolation. The apparatus used for this is called a pyranometer and measures the solar irradiance directly in power delivered per area exposed to the sun (W/m^2).

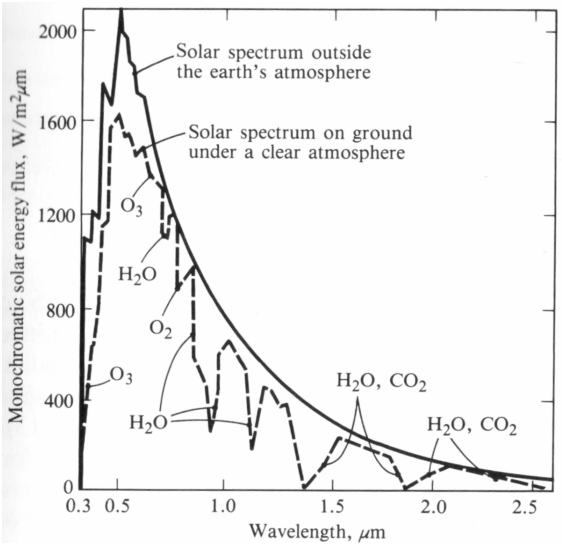

Figure 2.9: Solar spectrum (ref. 12)

The spectrum of the sun is shown in figure 2.9. Most of the light energy is transferred between 0.3 and 2.5 μm. These wavelengths are different from the heat radiation wavelengths with occur at wavelengths larger than 10 μm. The solar spectrum at sea level differs in shape from the Planck curve because the atmosphere absorbs some frequencies. If the sunlight travels a greater distance through the atmosphere, the absorption peaks will be more pronounced, and less energy will reach the collector. This effect is called air mass (AM). The shortest path through the atmosphere to sea level gives AM=1. Spectra taken at higher altitudes show less pronounced absorption peaks.

2.4.3 Spectrally selective surfaces

From the last two paragraphs it is concluded that the heat radiation losses and the solar radiation influx occur at different wavelengths. Therefore the absorption coefficient (also called absorptivity or absorptance) and the emission coefficient do not need to be the same. A spectrally selective surface is a surface with a large absorption coefficient and a small emission coefficient. Spectrally selective surfaces have been extensively investigated (ref. 13-37). They can be produced by electro deposition, chemical etching, painting, spraying, reactive spraying, sputtering, chemical vapor deposition, thermal oxidation, mechanical application and many more. They can posses absorption coefficients ranging from 0.9-0.98 and can have emission coefficients as low as 0.02. A typical normal reflection spectrum of a selective surface is shown in figure 2.10
:

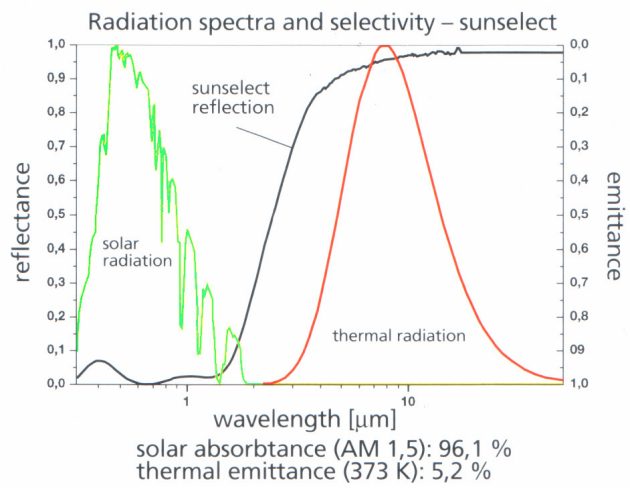

Figure 2.10: Normal reflection spectrum of a commercial selective surface (Sunselect) and thermal and solar radiation spectra.

Selective surfaces can improve the efficiency of solar boilers dramatically because most of the sunlight is absorbed and not much heat radiation occurs. Spectrally selective coatings rely on a number of physical phenomena like destructive interference between layers, semiconductor behavior, optical trapping and others. Combinations of these phenomena can be used. Some surfaces also utilize a transparent heat reflective coating on top of the selective surface.

The radiative properties of spectrally selective surfaces are dependent on the angle of incidence. If the angle of incidence is zero then the rays hit or emerge the absorber perpendicular (or normal). Typical dependencies are given in figures 2.11 and 2.12.

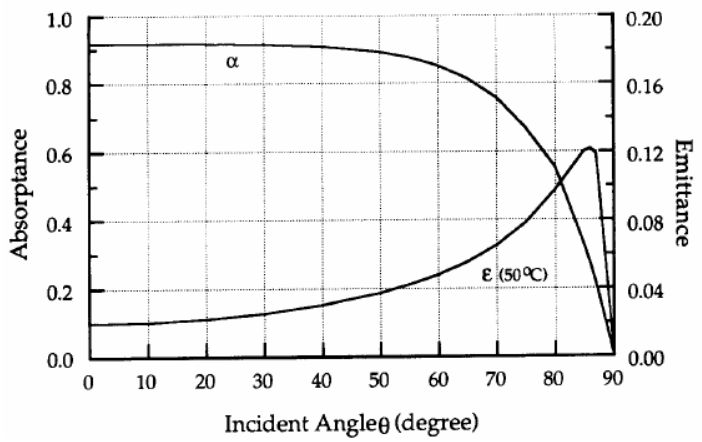

Figure 2.11: Typical incident angle dependency of radiative properties of a bi-sublayer selective surface (ref. 13)

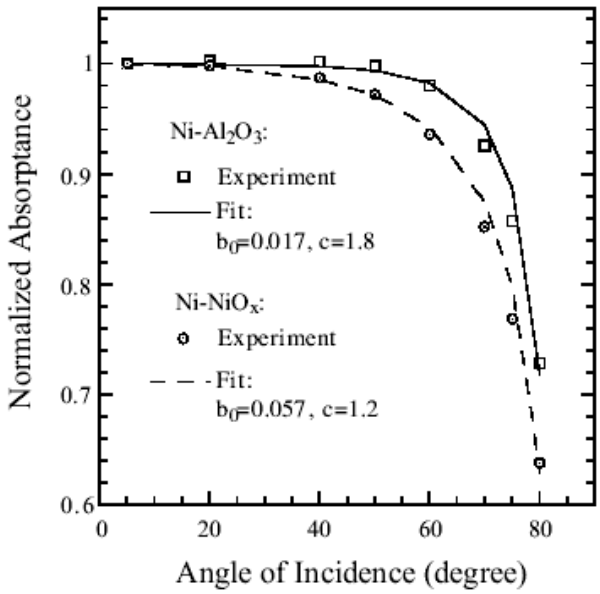

Figure 2.12: Typical incident angle dependency of a Ni-Al_2O_3 and Ni-NiO_x selective surface (ref. 14)

The figure shows that the perpendicular absorptance and emittance may not be suited to predict the collector efficiency. Instead the hemispherical absorptance and emittance should be used (because the boiler is a cylinder). The hemispherical properties are influenced by the surface roughness. Therefore it is not possible to calculate these properties from the normal properties only.

2.4.4 Cover radiation

The cover of a solar boiler also has some effect on the efficiency. Just like the absorber the cover affects both the solar radiation gain and the thermal radiation losses. The transparency of the cover for solar radiation is dependent on the incident angle, the refraction index of the cover material and the polarization. This transparency or transmittance can be calculated using formulae formulated by Fresnel (ref. 38). Because the sunlight is not polarized the average of the two Fresnel formulae is used. The refraction index of PVC is 1.52-1.55 (ref. 39). Using Fresnel's formulae the transparency as a function of angle of incidence was calculated and is shown in figure 2.13:

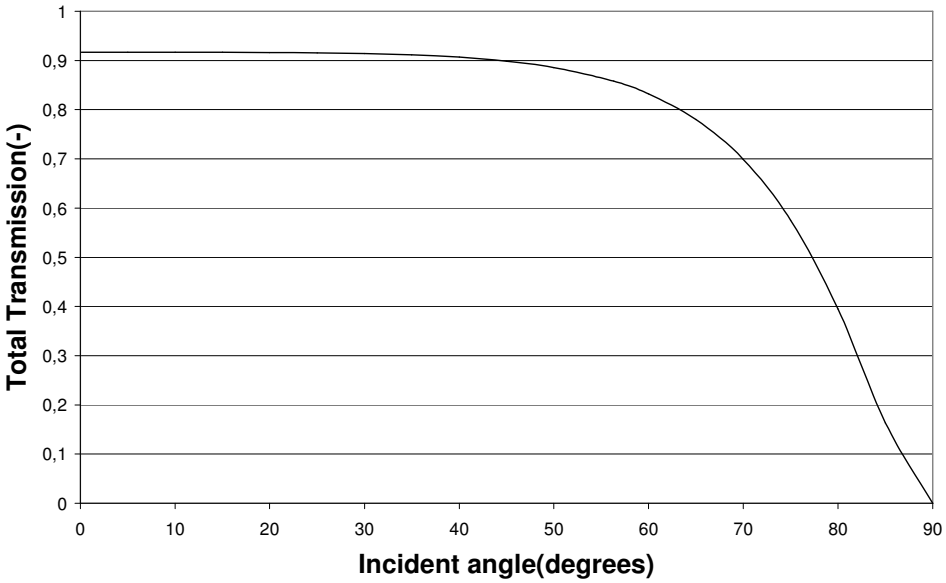

Figure 2.13: Light transmission of sunlight through PVC as a function of incident angle

As can be seen, the light transmission is fairly constant at incident angles under 40°. If the sun strikes the cover at an angle of over 40° much of the light is reflected. The design of the solar boiler should be such that the light that falls on the absorber shines through the cover with an incidence angle smaller than 40°.

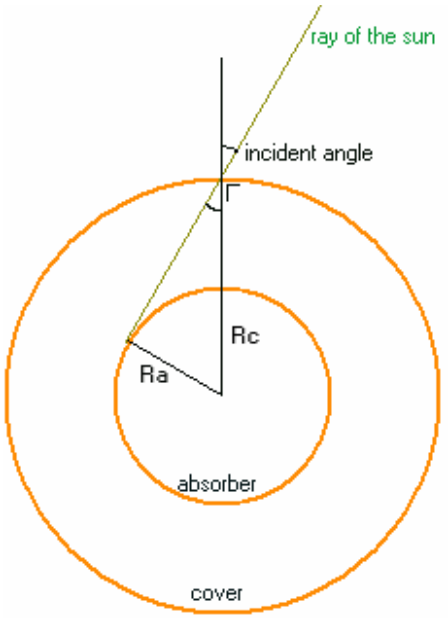

Figure 2.14: The radii of the absorber and the cover determine the maximum angle of incidence of the sunlight with the cover

The maximum angle at which the sun strikes the cover can be calculated (figure 2.14). A ray is drawn that strikes the absorber as far from the middle as possible. The maximum incident angle if this ray with the cover is:

$$\delta_i^{\max} = \sin^{-1}\left(\frac{R_c}{R_a}\right) \qquad \text{(Eq. 2.10)}$$

where:
δ_i^{max} Angle of incidence [^{o}]

The radius of the absorber was chosen to be 0.25 m and the radius of the cover 0.45 m, so that the maximum incident angle is 33.7^o resulting in a high hemispherical transmission coefficient.
The rotating solar boiler can be compared with an evacuated tube collector. An evacuated tube produced by *Apricus Solar Co. Ltd* has an R_a = 23.5 mm and R_c = 29 mm. The maximum incident angle is 54.1^o in this design. The collector is made of borosilicate glass that has a refractive index of n=1.47. Integrating τ from 0 to 54.13^o in the Fresnel formulae yields that the total hemispherical transmission coefficient τ_h= 0.921 for the evacuated tube collector.
For prototype 2 and 3 the PVC cover has n=1.52 and δ_i^{max} =33.7^o. This yields a total hemispherical transmission coefficient of τ_h= 0.916.

2.4.5 The reflectors

The reflectors supply a lot of light to the absorber. Mirrors can be made from many different metals. In table 2.1 the reflectivity (*r*) of some surfaces is given.

Table 2.1: emission coefficients and reflection coefficients of various surfaces (ref. 40)

Material	*Emission coefficient*	*Reflection coefficient*
Oxidized galvanized steel	0.276	0.724
Polished zinc	0.045-0.053	0.955-0.947
Aluminum polished	0.039-0.057	0.961-943
Aluminum surfaced roofing	0.216	0.784
Polished gold	0.018-0.035	0.965-0.982
Aluminized polyester film (value from manufacturer)	0.2	0.8

Mirrors that are exposed to the elements cannot be expected to stay polished. Dust and wind will quickly reduce the reflectivity. Therefore it is not good practice to resort to the high-end reflectors for solar applications if the reflectors are not covered by glass. Aluminized polyester film is a reasonably effective reflector and was used for all the prototypes. The reflectivity of aluminized polyester depends on the angle of incidence as can be seen in figure 2.15:

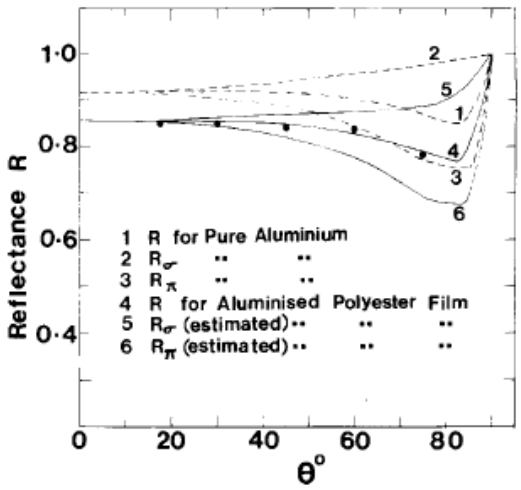

Fig. 2. Specular reflectance R (experimental) for aluminised polyester film as a function of angle of incidence (—●—●—). The σ and π components for the aluminised polyester, estimated from the theoretical reflectance data for pure aluminium, are shown as solid lines. The dashed lines show the reflectances of pure aluminium (total, σ and π components) calculated from tabulated data[20].

Figure 2.15: Experimental and theoretical reflectance of aluminum and aluminized polyester as a function of the angle of incidence (ref. 41)

From figure 2.15 it becomes apparent that the assumption that the reflectivity is constant over all angles of incidence is not strictly correct. However, an average value of 0.8 was used in the model.

2.4.6 Reflector geometry

The reflector geometry is of crucial importance to the overall yield of the collector. Cylindrical absorbers without reflectors are always partially shaded. The mirrors can compensate for this by using sunrays that will miss the absorber and reflect them onto the backside and the bottom of the absorber.
If the collector is made to trace the sun, the simple analytical solution is to use a parabolic mirror. With stationary mirrors however there is no definite solution. Some research has been done on stationary reflectors (ref. 41 - 43). The most efficient shape and size of the reflector depend on the latitude, on the height of the sun and on the heat loss of the collector. It is also expected that the sun will be obscured by clouds more at lower sun angles. A trade off will have to be made.
The concentration factor of an ideal reflector (*m*) is defined as the power reflected onto the absorber divided by the power directly irradiated onto the absorber. Generally, a concentration factor of 3 can be achieved. In order to choose a suitable shape a ray-tracer program was written (see appendix 2). This program calculates the concentration factor as a function of the incident angle of the sun for a given reflector shape.

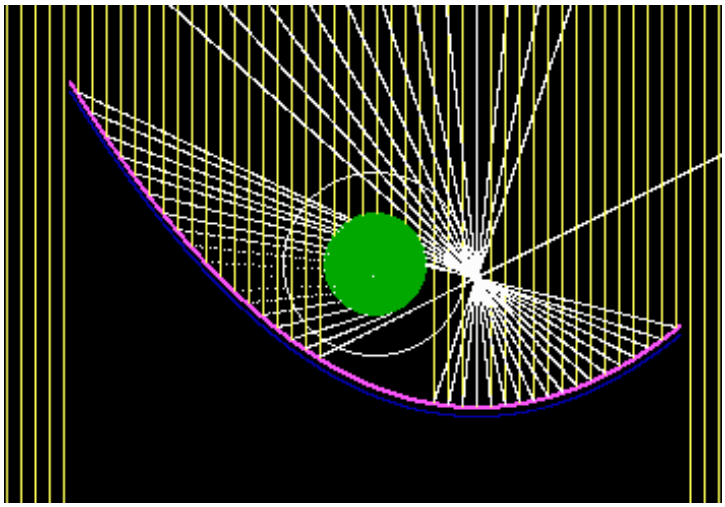

Figure 2.16: Visualization of the paths of the sunrays. The absorber is green and the reflector is purple. The sunrays are yellow and the reflected rays are white.

Although the program is able to evaluate reflector geometry, the geometry has to be chosen first. There are an infinite number of shapes that can be used. Several options were evaluated and the results are plotted in figure 2.17:

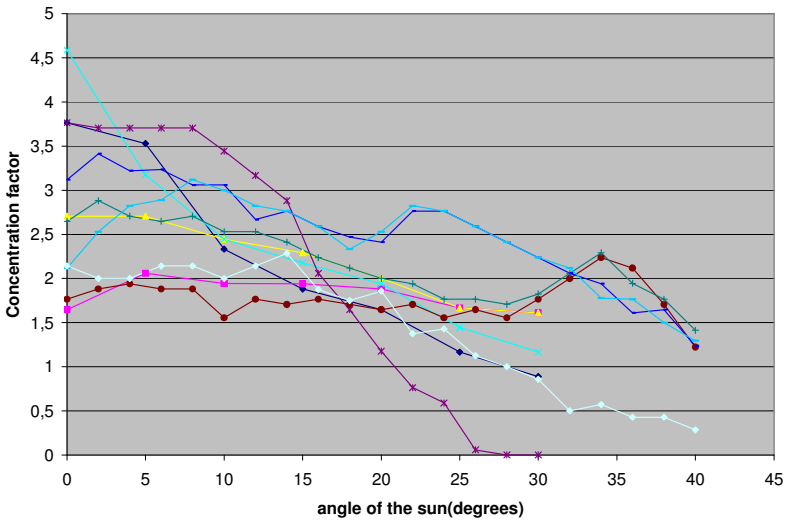

Figure 2.17: Concentration factors as a function of the angle of the sun for reflectors of different sizes and geometries

The different geometries can give a wide range of concentration factors as a function of the angle of incidence. For this research a constant concentration factor as a function of angle is more desired than a high concentration factor. As can be seen in the figure these geometries do exist.

2.5 Mechanical losses

The collector has to be rotated in order to prevent convection. This requires mechanical power. The centrifugal force needs to exceed the gravitational force. The speeds that are required are generally small (see paragraph 2.3.1) and hence the drag is small.
The mechanical losses are extremely difficult to calculate because of the wind. Wind varies and effects are hard to predict. It is even possible that the wind rotates the absorber by itself yielding a negative electrical loss.
For prototype 1 the velocity of the cover exceeded 1.9 m/s. The power the motor consumed during operation was 8W. This is very small as compared to the 0.5 kW design heat gain. The first prototype's mechanical construction was fairly poor, thus it can be expected that the electrical power consumption is even less.

2.6 The model

In the previous paragraphs the contributors to the efficiency of the collector are described. The maximum power that enters the system is:

$$\Phi^{in} = \Phi^{"in} \cdot A_i \cdot (1+m) \qquad \text{(Eq. 2.11)}$$

with:

Φ^{in}	Power input of the sun	[W]
$\Phi^{"in}$	Solar influx	[W/m^2]
A_i	Illuminated absorber area	[m^2]
m	Concentrating factor of the reflector	[-]

In order to predict a rotating boiler's heat production an energy balance was set up:

$$\Phi^{prod} = \Phi^{"in} \cdot A_i \cdot \tau_h \cdot \alpha_{a,h} \cdot (1+m \cdot r) - \Phi^{cond} - \Phi^{conv} - \Phi^{rad} \qquad \text{(Eq. 2.12)}$$

with:

Φ^{prod}	Rotating solar boiler heat production	[W]
$\Phi^{"in}$	Solar influx	[W/m^2]
A_i	Illuminated absorber area	[m^2]
τ_h	Hemispherical transparency of the cover	[-]
$\alpha_{a,h}$	Hemispherical absorption coefficient of the absorber	[-]
m	Concentrating factor of the reflector	[-]
r	Reflection coefficient of the reflector	[-]
Φ^{cond}	Conductive heat loss	[W]
Φ^{conv}	Convective heat loss	[W]
Φ^{rad}	Radiative heat loss	[W]

The heat losses Φ^{cond} and Φ^{rad} are quantitatively described in paragraphs 2.2 and 2.4, whereas the Φ^{conv} is set to zero (see paragraph 2.3).

The theoretical efficiency η can be calculated using equations 2.11 and 2.12:

$$\eta = \frac{\Phi^{prod}}{\Phi^{in}} \qquad \text{(Eq. 2.13)}$$

The optical efficiency η_0 (or ambient temperature efficiency) is the measure for the fraction of the incoming light that is converted into heat without taking into account any heat loss:

$$\eta_0 = \frac{\Phi^{"in} \cdot A_i \cdot \tau_h \cdot \alpha_{a,h} \cdot (1+m \cdot r)}{\Phi^{in}} = \frac{\tau_h \alpha_{a,h} (1+m \cdot r)}{(1+m)} \qquad \text{(Eq. 2.14)}$$

If no reflectors are used, equation 2.14 reduces to:

$$\eta_0 = \tau_h \alpha_{a,h} \qquad \text{(Eq. 2.15)}$$

The theoretical efficiency of prototype 3 is calculated using the parameters from table 2.2. It should be noted that the normal properties are used instead of the hemispherical properties, since these values were provided by the manufacturer of the selective coating.

Table 2.2 Parameters that determine the efficiency of prototype 3

Parameter name	*Symbol*	*Value*	*Units*
Absorber radius	R_a	0.25	m
Cover radius	R_c	0.45	m
Absorber length	l	1.2	m
Hemispherical emittance of the absorber	$\varepsilon_{a,h}$	$\varepsilon_{a,n} = 0.052$	-
Hemispherical absorptance of the absorber	$\alpha_{a,h}$	$\alpha_{a,n} = 0.961$	-
Hemispherical transparency of the cover	τ_h	0.916	-
Ambient temperature (cover temperature)	T_c	298	K
Operation temperature (absorber temperature)	T_a	373	K
Number of mirrors	m	2	-
Reflectivity of the mirrors	r	0.8	-
Solar heat flux	Φ''^{in}	800	Wm^{-2}
Heat transfer coefficient of end caps	λ_e	0.027	W/(m·K)
Thickness of end caps	d_e	0.08	m
Heat transfer coefficient of air	λ_{air}	0.0298	W/(m·K)

At a design temperature of 100°C the radiative losses can be calculated using equation 2.7. This yields Φ^{rad} = 64 W. The conductive losses are determined with equations 2.1 and 2.2. The total conductive losses are Φ^{cond} = 61 W. It is assumed that there are no convective losses (Φ^{conv} = 0 W). From equation 2.12 the heat production of the solar boiler becomes Φ^{prod} = 974 W. Applying equations 2.13 and 2.11 gives a theoretical efficiency of η = 69%. This efficiency cannot be reached because the normal properties of the selective surface are better than the hemispherical properties. In order to obtain reasonable estimates for the hemispherical optical properties data from evacuated tube collectors can be used.

Commercial evacuated tube collectors have identical geometries and comparison with the proposed design is easy. In evacuated tubes only radiative losses occur. The efficiencies of evacuated tube collectors as a function of temperature and insolation are given by the manufacturers. In figure 2.18 these curves are shown as well as the model for the rotating solar collector with normal radiative properties (purple line). The first evacuated tube is produced by *Apricus Solar Co. Ltd* (orange line, ref. 1) and does not have any reflectors. The other system (green line, ref. 7) is the *Ritter CPC evacuated tube collector*, which has reflectors.

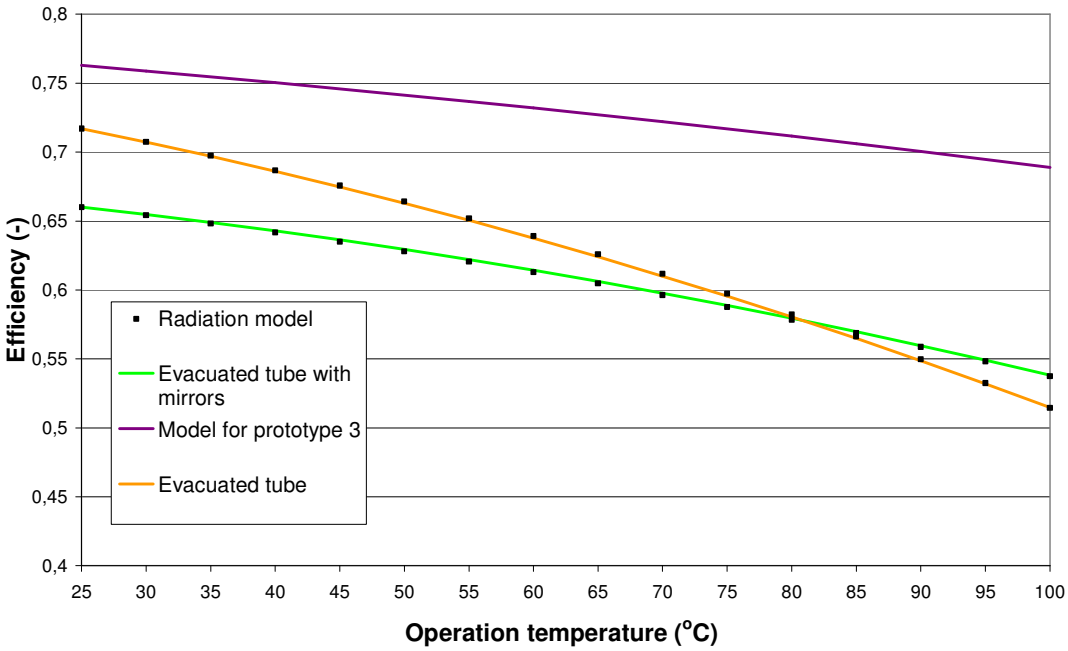

Figure 2.18: Efficiencies of solar collectors as a function of operation temperature. T_0=25^{0}C; insolation 800W/m^2

The efficiency curves of the evacuated tubes are used to obtain reasonable values for the hemispherical absorptance and emittance. These curves are fitted to a simple radiation only model:

$$\eta = \eta_0 - \frac{\varepsilon_{a,h} \cdot \sigma \cdot \left(T_a^4 - T_c^4\right)}{\Phi''^{in}} \quad \text{(Eq. 2.16)}$$

This yields values for the optical efficiency η_0 and the hemispherical emissivity $\varepsilon_{a,h}$, which are given in table 2.3.

Table 2.3: Hemispherical radiative properties of commercial evacuated tube collectors

Manufacturer data	*Apricus*	*Ritter*
η_o	0.717	0.661
$\varepsilon_{a,h}$	0.079	0.048

The radiation model (equation 2.16) with the values from table 2.3 are shown as black dots in figure 2.18. It can be seen that the model is appropriate, because the efficiencies coincide. The values for the hemispherical emission coefficients $\varepsilon_{a,h}$ are similar to the normal value of the selective surface given by the manufacturer (see table 2.2). Therefore, using the normal emission coefficient instead of the hemispherical emission coefficient does not lead to large deviations in the model.

It can be concluded that the hemispherical emission coefficients $\varepsilon_{a,h}$ of the commercial tubes are correct. The main deviation stems from the difference in hemispherical and normal absorption coefficients $\alpha_{a,h}$.
It is possible to calculate the absorbtivity $\alpha_{a,h}$ of the Apricus collector (ref. 1). Because it has no reflectors, equation 2.15 can be applied. The hemispherical transmisivity τ_h of the cover of the Apricus collector can be calculated using the Fresnel formulae, the index of refraction of borosilicate glass (n) and the radii of the two tubes (R_c and R_a). These values are n = 1.47 (ref. 44), R_a = 47mm and R_c = 58mm. The hemispherical transmission becomes τ_h = 0.92. This yields a hemispherical absorption coefficient $\alpha_{a,h}$ = 0.717/0.92 = 0.78. The hemispherical absorption coefficient ($\alpha_{a,h}$ = 0.78) is much lower than the normal absorption coefficient ($\alpha_{a,n}$ > 0.92) given by the manufacturer (ref. 1). If the assumption is made that the rotating solar boiler also has a hemispherical absorptivity of $\alpha_{a,h}$ = 0.80 instead of $\alpha_{a,n}$ = 0.961, then the adapted model can be plotted again (purple line in figure 2.19).

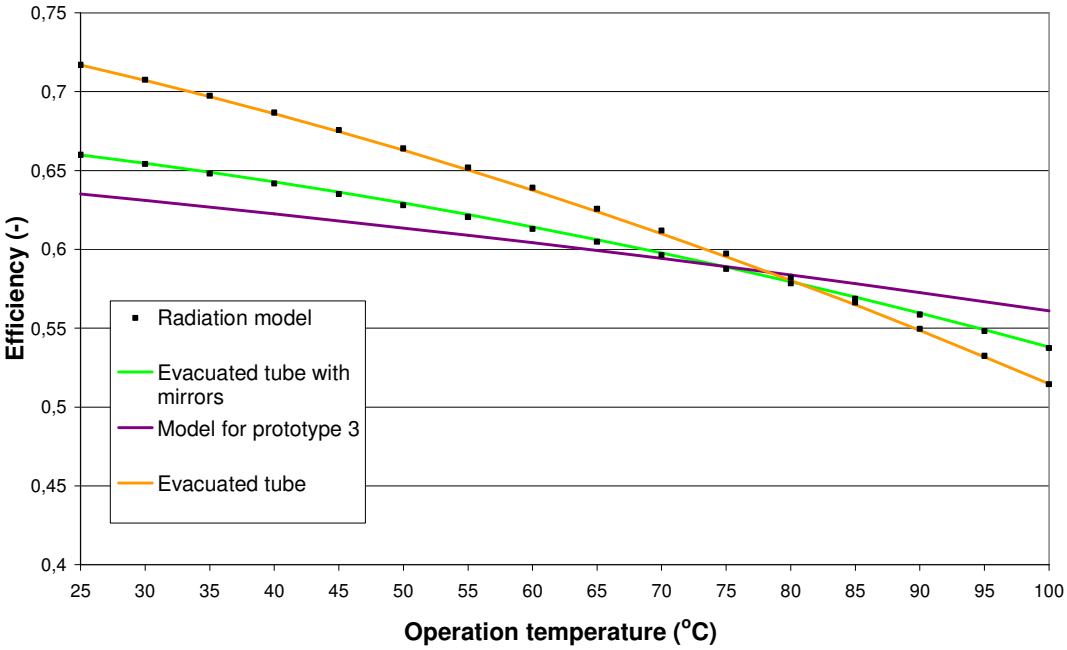

Figure 2.19: Model for prototype 3 with α_h=0.80 compared with commercial evacuated tube collectors; insolation = 800 W/m^2 and T_0 = 25°C

In this case, the efficiency of the rotating solar boiler is comparable to evacuated tube collectors. At an insolation of 800 W/m^2 and an ambient temperature of 25°C, an efficiency of 56% is predicted (instead of an efficiency of 69% when normal optical properties of the selective surface are used). Experiments were done to test this model.

2.7 Economic evaluation

In order to establish the economic feasibility two approaches can be used. The first approach is to compare a solar collector with fossil fuel. The second approach is to compare the cost of a rotating solar boiler with the cost of other solar collectors.
If fossil fuel is going to be replaced with sustainable solar energy an economic evaluation may be made. However there are unknowns regarding the future energy price and the weather. Therefore it is difficult to predict a pay back time. The second approach is much easier. The material costs of several collectors may be compared. The relative material costs of common solar collector materials are listed in table 2.4 (ref. 45):

Table 2.4: Relative costs of solar collector materials (ref. 45)

Material	*Relative cost (/kg)*
Aluminum 6061 sheet	7.6
Copper C11000 sheet	7.9
Glass soda lime plate	2.9
Borosilicate glass (Pyrex)	18.2
Polycarbonate sheet	12.1
PTFE sheet	54

The material costs of different solar collectors are compared: a flat plate collector, a vacuum tube collector and the rotating solar collector.
A typical flat plate collector (ref. 46) weighs 18 kg/m^2 illuminated absorber area. It has a 4 mm thick glass cover. This cover weighs 10 kg/m^2. The remaining 8 kg/m^2 is aluminum and copper used for the absorber, the piping and the frame. The relative cost of such a system is $10 \cdot 2.9 + 8 \cdot 7.6 = 90/m^2$.
A vacuum tube collector consists entirely of Pyrex glass. The weight of such a system is about 25 kg/m^2 (ref. 1). The relative cost thus becomes $25 \cdot 18.2 = 455/m^2$.
Prototype 3 consists of a copper absorber (ρ_{Cu} = $8.96 \cdot 10^3$ kg/m^3) with a radius of R_a=0.25m, a length of L=1.2m and a thickness of d_a=0.20mm. The weight of the absorber is $2 \cdot \pi \cdot R_a \cdot L \cdot d_a \cdot \rho_{Cu}$ = 3.4 kg. The cover tube has a radius of R_c=0.45m and a thickness of d_c=0.10mm. The cover should not be made from PVC because it is not resistant against UV radiation and will degrade. Therefore a UV resistant transparent polymer like PC, ETFE or PTFE should be used. The non-fouling properties of ETFE and PTFE may be preferred. If PTFE (ρ_{PTFE} = $2.2 \cdot 10^3$ kg/m^3) is used, the weight of the cover is $2 \cdot \pi \cdot R_c \cdot L \cdot d_c \cdot \rho_{PTFE}$ = 0.7 kg. The illuminated absorber area is A_i = 0.6m^2. Thus, the weight per square meter becomes: (3.4 + 0.7)/0.6 = 6.8 kg/m^2 and the relative cost is $(3.4/0.6) \cdot 7.9 + (0.7/0.6) \cdot 54 = 110/m^2$. If a rotating boiler is constructed using a cover of 0.10 mm Polycarbonate and an absorber consisting of 0.10 mm copper, the relative price becomes 38/m^2.
Overviews of the relative costs are listed in table 2.5.

Table 2.5: relative material cost comparison of different types of solar collectors

Collector type	*Relative cost [m^{-2}]*
Flat plate collector	90
Evacuated tube collector	455
Rotating solar boiler	38-110

This analysis does not take into account the equipment needed to run the collectors. This is expected to be somewhat higher for the rotating solar boiler because bearings and a motor are required. The other collectors only require a pump. The analysis also shows very clearly that solar boilers should have a very low weight. If less material per surface is used the pay back time is shorter. Because the solar boiler works at atmospheric conditions, it can be lighter and cheaper than evacuated tube collectors.

3. Experimental, results and discussion

In this chapter it is described how the prototypes were constructed and operated. The construction and operation then yields information to meet the 4 research goals. The research goals are:

1. Select suitable materials for the boiler
2. Develop a model in order to predict the performance of rotating solar boilers
3. Evaluate the efficiency of the solar boiler
4. Economic evaluation

An iterative approach was chosen to meet the goals. Because all the goals are interrelated they should be looked at simultaneously. The results and conclusions of the first prototype were used for the construction of the second prototype and so on. Every iteration gives more insight in the model, the materials needed, the performance of the boiler and the economics of the system. The three iterations made during the research are described as well as the choices made for the next iteration based on the results.

3.1 Prototype 1

Prototype 1 was made in spare time and with own resources. The lack of resources introduced some unknowns but the experiment is described for completeness.

3.1.1 Experimental

Prototype 1 was constructed using a dented galvanized steel tube with a length of 1.0 meter, a diameter of 0.32 meter and a wall thickness of 0.6 mm. The solar selective surface consisted of a soot layer applied with a flame. Research indicates that thin carbon layers deposited on a metallic infrared reflector yields spectral selectivity (ref. 30). The cover was made of a recycled transparent polymer film.

In figure 3.1 the absorber is shown. As can be seen it is already partly blackened by a flame.

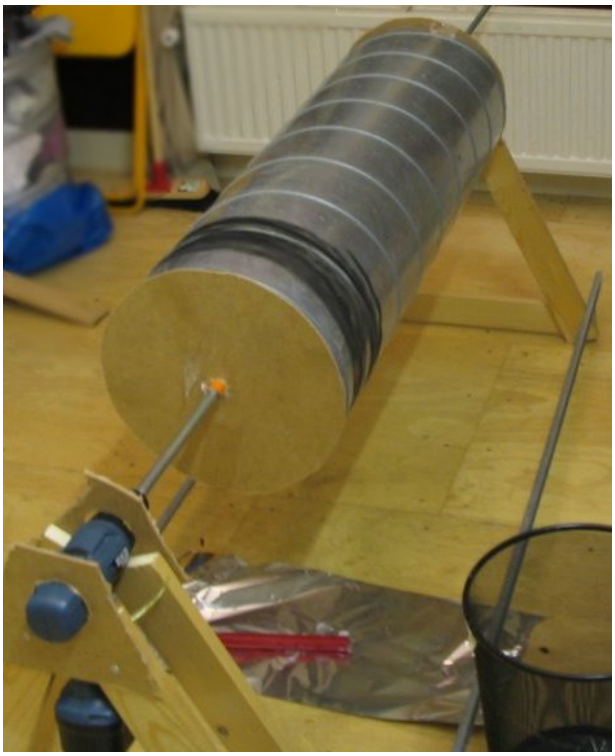

Figure 3.1 picture of the unfinished absorber in its frame

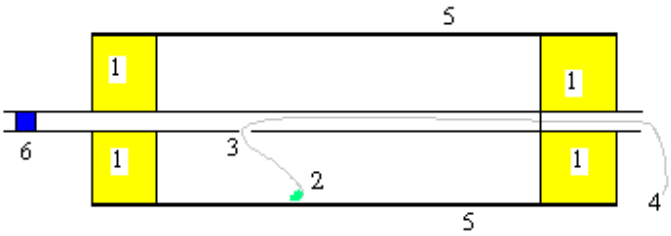

Figure 3.2: Schematic overview of absorber construction

The parts of the absorber are:

1. PUR foam
2. Waterproof temperature sensor NTC - 100kΩ @ 25°C
3. Hole in axle
4. Connection wire for temperature sensor
5. Absorber tube (galvanized steel tube, L = 1.0m and D = 0.32m)
6. Silicon rubber in axle

The foam keeps the absorber in its place and insulates the inside. The inside contains a temperature sensor (NTC) that has been waterproofed with silicon rubber. The hole in the axle allows the wire for the sensor to go to the outside. Furthermore the hole allows water to enter and steam to escape. One side of the axle is filled with rubber (6) so steam only exits from one side.

After the absorber had been constructed the cover was added as can be seen in figure 3.3

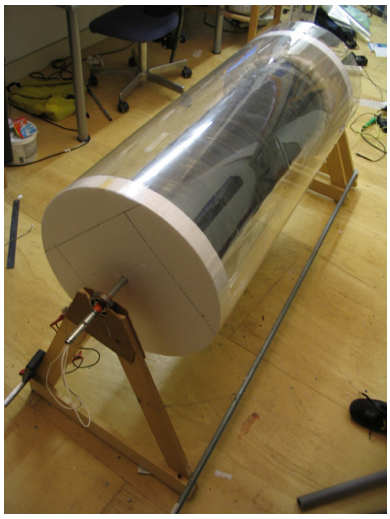

Figure 3.3: Cover is added

In order to fasten the cover two polystyrene foam disks were fixed to the absorber. The outside diameter is 0.50m. The cover is a transparent hard plastic foil like those used for overhead projector sheets. The cover is fixed to the foam disks with tape.
The temperature sensor is measured using a multimeter. The sensor rotates with the collector so brushes were made to keep the multimeter stationary.

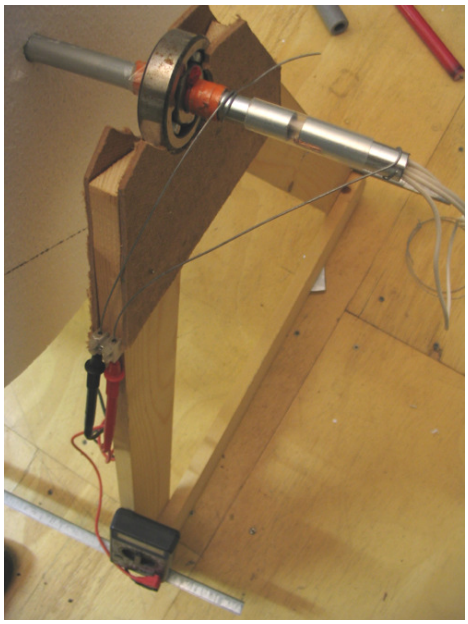

Figure 3.4: Brushes

In figure 3.4 you see the axle is sawn into two pieces connected with a plastic tube. The poles of the rotating NTC are connected to the multimeter (in the bottom). Excess wire can be seen.

Figure 3.5: Steam exits the axle during operation

The collector was operated without reflectors and without water. The operation temperature (100^{o}C) could not be established without the reflectors. Two tests were done and a maximum temperature of 85 ^{o}C was measured. This result was beneficial because it proved that the absorber surface was somewhat spectrally selective.

Figure 3.6: Reflectors increase the power input of the collector

The prototype was put outside in the sun and allowed to heat up with the motor running. Rotation speed was determined and set to the correct speed. The power consumption of the motor was established at 8W at 75 RPM. When the temperature sensor indicated that the temperature began approaching 100^{o}C water was poured in through the axle. After a

while steam began to evolve from the axle. A problem was that the PUR foam proved to be leaking some steam. This steam condensed on the cover making it less transparent. This decreased the efficiency. When the motor was stopped steam evolvement stopped as well and the temperature began to decline. This was done at a constant solar irradiation proving the rotation prevented convection and increased efficiency.

3.1.2 Economic evaluation

The prices for the different parts were estimated (table 3.1):

Table 3.1: Prices for the different parts of prototype 1

Part	*Price (€)*
Absorber	80
Insulation	11
Reflectors	10
Motor	20
Bearings	5
Cover	10
Selective coating	2
Frame	30
Total	**168**

The total price of the collector is estimated to be € 168 (including BTW). The total illuminated area including the reflectors is 1.0 m^2, so the price per area is 168 euro per square meter. Because the efficiency was not established no pay back time could be calculated.

3.1.3 Results and discussion

Several important conclusions can be drawn from the experiments and the model.

1. Rotation prevents convection in the air layer.
2. The electrical power consumption is not prohibitive.
3. The carbon layer is indeed selective. Furthermore visual inspection proves the absorption coefficient increases with increasing angle of incidence.
4. The boiler needs to be steam proof in order to prevent condensation of water on the inside of the cover.
5. Efficiency should be measured.
6. The boiler has enough potential to justify further investigation.

3.2 Prototype 2

The second prototype was constructed to do quantitative measurements. It was attempted to make the boiler as big as possible because the model indicates that the efficiency could benefit. If the length is larger, the relative cost for end caps and bearings is less. If the diameter is bigger, the relative area of the absorber to the cover becomes larger. It was also presumed that a bigger boiler would generate more steam and hence it would be easier to do precise measurements.

3.2.1 Experimental

Prototype 2 was constructed using an absorber of galvanized steel. The tube length was 3.0 meter, the diameter was 0.50 meter and the thickness was 0.6mm. Solkote® selective paint was applied on the tube. The cover was made of transparent PVC film. The shape of the cover was maintained by a slight overpressure (<200 Pa). The overpressure was supplied through the axle with a small rotary pump. The cover diameter was 0.90 meter.
Instead of using a temperature measurement the steam flow was measured. Because saturated steam flows are difficult to measure directly, all the steam was condensed and weighed. The condenser was a water-cooled all glass condenser. The scale was a Sartorius® with a precision of 0.1 gram. The insolation was measured using a pyranometer (GS-WV) obtained from Wittich & Visser. The pyranometer was installed at an angle of 45^{o} from the horizontal plane and parallel to the absorber tube. A temperature sensor was introduced in the axle where the steam evolves. Reflectors were added behind and below the boiler. The concentration factor was 2 yielding a total collector area of 4.5 m^2. The boiler was started up with and maintained at a rotation speed of 60 RPM. The collector was loaded with water until the power output stabilized. The loading was 8.0 kg of tap water. No condense was seen on the cover. This indicates that the absorber was steam proof. For some hours the solar irradiance and the weight of the steam were measured.

Figure 3.7: Prototype 2

3.2.2 Economic evaluation

The material costs of prototype 2 are much better documented than the first prototype. This is because most of the materials were bought. The material costs are listed in table 3.2

Table 3.2: Material cost for prototype 2

Item	*Cost (€)*
Cover	18.18
Absorber tube with end caps	169.04
Frame	68.85
Bearings	74.40
Insulation	103.90
Reflectors	35.22
Motor	25
Selective paint	2
Total	**496.59**

The motor was loaned from the Laboratory for Process Equipment, where the rotation speed can be set. This 750 W motor is too big for the boiler. The boiler could also be started and driven by a 12 V 20 € drill.
The total material cost is €469.59 for an effective area of 4.5 m^2. The cost per area is 104.35 €/m^2 including taxes (19 %BTW). The material costs without taxes is 417.30 € and the material costs per square meter without taxes is 92.73€/m^2.

3.2.3 Results and discussion

The measurements were plotted in figure 3.8

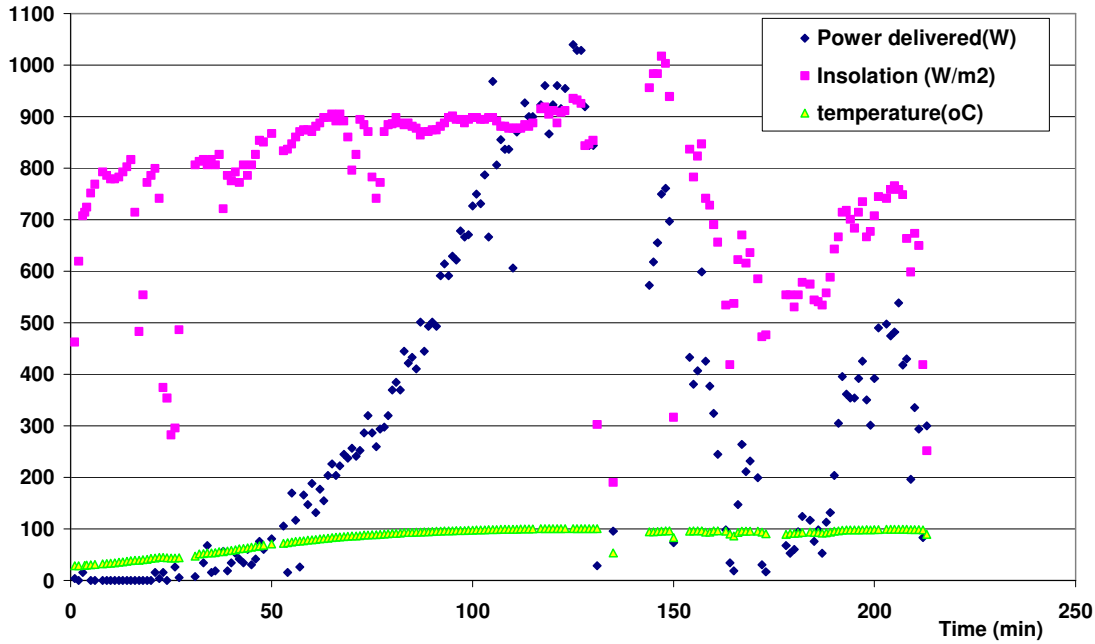

Figure 3.8: Performance of prototype 2: Solar irradiance (W/m^2), temperature (^{o}C) and produced steam (W) in time T_0=19^{o}C

From the graph it can be concluded that the large water mass leads to a long heat up time. It can also be concluded, that the temperature sensor is not located correctly. It does not measure the absorber temperature and hence cannot be used to calculate the efficiencies at temperatures lower than the operation temperature of 100^{o}C. The steam mass measurements have a considerable uncertainty. This is due to the effect of the wind on the scale.
From the graph (figure 3.8) it becomes apparent that the intensity of the sunlight decreases after about 150 minutes of measurements. This is fortunate because the efficiency can be calculated at different insolations (figure 3.7).

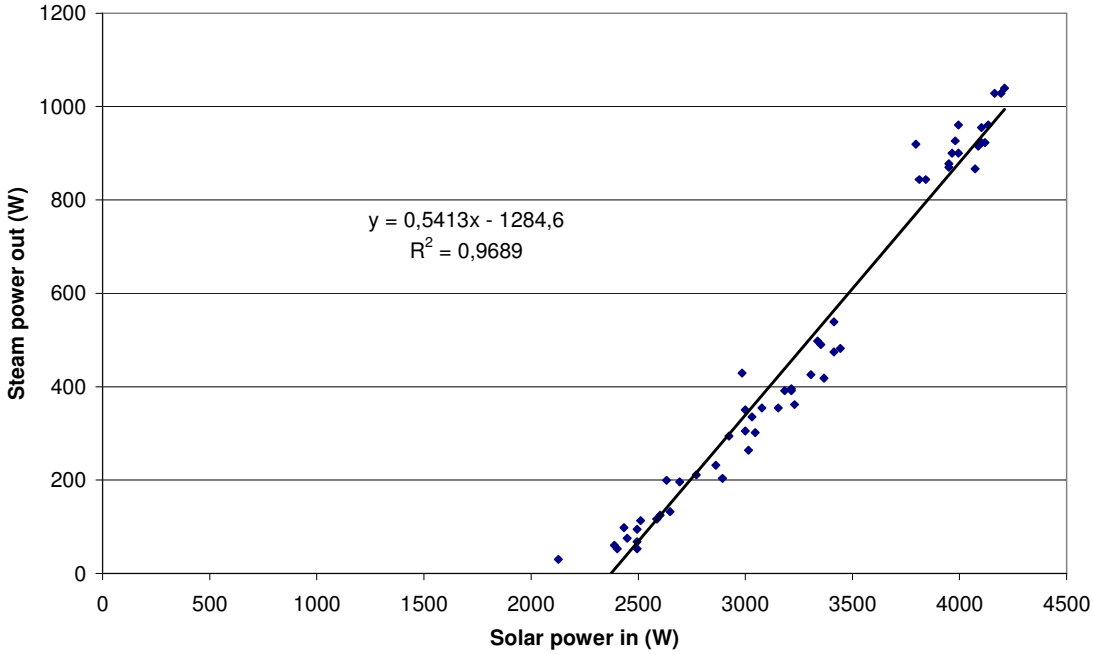

Figure 3.9: Steam delivered (W) as a function of the solar irradiance (W)

Figure 3.9 was constructed using the data points that were not affected by the wind too much. From the graph it becomes apparent that the optical efficiency is $\eta_0 = 54\%$ (slope). The total heat loss at 100°C is 1.3 kW (offset). The maximum measured efficiency for prototype 2 is $\eta = 25\%$ (max. solar power in divided by max. steam power out).
The emission coefficient and the absorption coefficient are the only two unknown variables and can be calculated using the slope and the offset. Using equation 2.14 this gives for the absorption coefficient α_h=0.70. Using equations 2.1, 2.2 and 2.7 emissivity of the absorber is calculated, yielding ε_h=0.30. These optical properties are very poor. However other effects may have taken place that decreased the efficiency of the rotating boiler such as a misalignment of the mirrors.
The manufacturer of the paint has indications for the optical properties of their product on copper and aluminum substrate. However no data is available for galvanized steel substrate. The emissivity of the paint can range from 0.28 - 0.49, and absorption coefficient from 0.88 - 0.94. Thus the measured absorption coefficient is less than the specifications.
This indicates that there is another effect that decreases the optical efficiency of the boiler. Too little variables are known for this boiler to investigate this effect. It was concluded that a selective surface with better-defined optical properties was needed to quantify this effect.
Another conclusion was that the water loading was high. The thermal mass of the boiler becomes very high with high water loadings and this has negative effect on the non-steady state operation of the boiler. The high water loading needed is caused partially by a dent in the tube and partially by the surface properties of the inside of the galvanized tube. It was observed that the galvanized surface does not wet easily. Droplet formation

occurs. After the initial high water loading of water the efficiency remained constant even at lower water loadings.
After the experiments were conducted the inner tube was inspected (figure 3.10).

Figure 3.10: Scaling inside the absorber tube.

Scaling occurred due to precipitation of the dissolved salts in the tap water. This scaling provided a hydrophilic layer. The complete layer was moist. It was concluded that the scaling benefits the wetting of the tube and provides an easy method to keep the water loading and the thermal mass of the boiler limited.

3.3 Prototype 3

From prototype 2 it was concluded that the selective surface was the main reason that the efficiency was fairly low. Therefore a better surface was obtained from Alanod Sunselect®.

3.3.1 Experimental

A tube was made from the coated copper band as can be seen in figure 3.11.

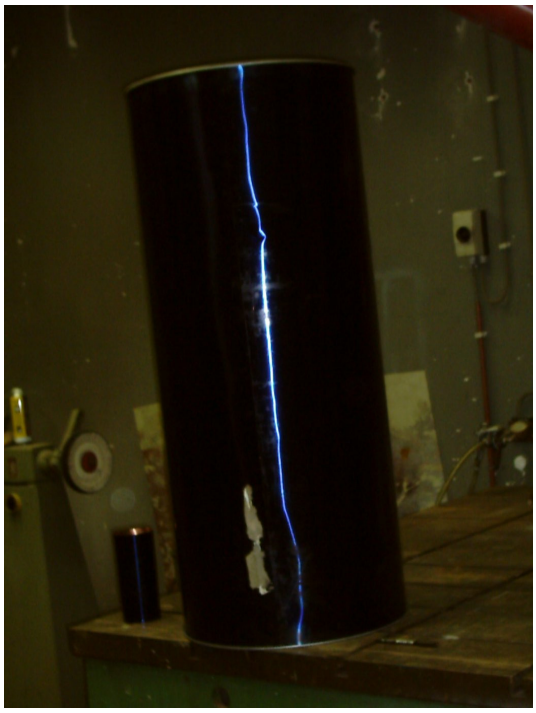

Figure 3.11: Tube made of coated copper

The tube is 1.2m long and has a diameter of 0.50m. The copper band was soldered to itself. There appeared to be some leaks due to the expansion of the copper during soldering. These leaks were closed using a sealant Adheseal® produced by Innotec. This procedure had a negative impact on the coating. In the picture some stains can be seen. These stains could not be removed with water, ethanol or acetone.
After the tube was constructed it was mounted in the modified frame of prototype 2 as can be seen in figure 3.12.

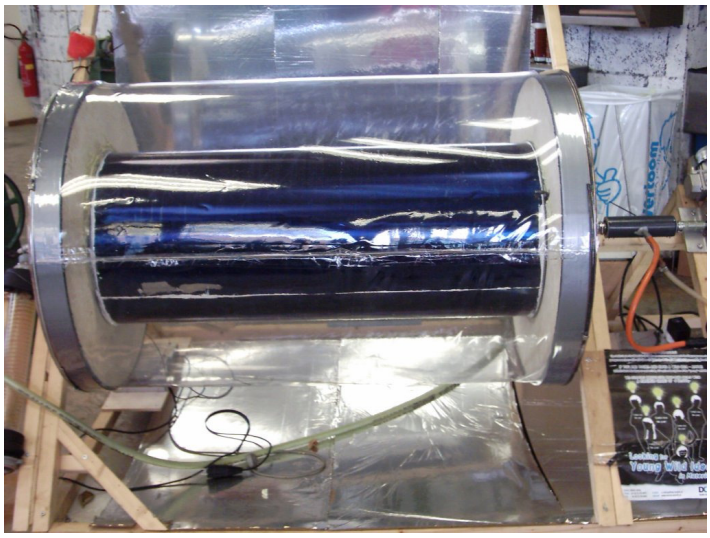

Figure 3.12: Completed prototype 3

The first tests were done in the beginning of October. The initial results were disappointing. Further investigation led to the conclusion that the lower reflector was not aligned properly. This may have been due to the low sun. The alignment of the reflector was identical to prototype 2. Therefore the performance of prototype 2 may not have been measured properly.

3.3.2 Economic evaluation

The economic evaluation for prototype 3 was made. Because the copper band was a gift no costs were made. Hence a different approach was sought to estimate the cost. A different manufacturer (European Solar Engineering) of a similar product has a cost calculator online (ref. 46). This tool suggests a price of 17.22 €/m^2 (excl. BTW, February 1st, 2006). The cost of the absorber would become 32.45 € excl. BTW.

Table 3.3: Material cost for prototype 3

Item	*Cost (€)*
Cover	7.27
Absorber tube with end caps	76.82
Frame	68.85
Bearings	74.40
Insulation	103.90
Reflectors	14.09
Motor	25
Total	**370.33**

The price of prototype 3 is € 370.33 (incl. BTW). The total aperture area (including reflectors) becomes 1.8m^2. The cost per surface area is 205.74 €/m^2. It can be easily seen that this boiler is too expensive to become feasible. However the bulk of the material cost stems from components that do not depend on the size of the collector. The coated copper tube is cheaper than the galvanized steel tube used for prototype 2. The copper tube costs estimation is 27.05 €/m (excl. BTW) and the galvanized steel tube costs 30.79 €/m (excl. BTW). If a boiler with the same dimensions as prototype 2 was constructed the material costs would be € 465.76 (see table 3.4).

Table 3.4: Material cost for a boiler with a 3.0 meter long copper tube

Item	*Cost (€)*
Cover	18.18
Absorber tube with end caps	140.21
Frame	68.85
Bearings	74.40
Insulation	103.90
Reflectors	35.22
Motor	25
Total	**465.76**

The total costs of this boiler would become € 465.76 (incl. BTW). The resulting aperture are is 4.5 m^2 and the cost per square meter would become 103.50 €/m^2.

3.3.3 Results and discussion

During the measurements adverse weather conditions limited the quality of the data obtained. Clouds obscured the sun and the wind caused the scale to fluctuate. However an attempt was made to obtain some measurements. These are plotted in figure 3.13.

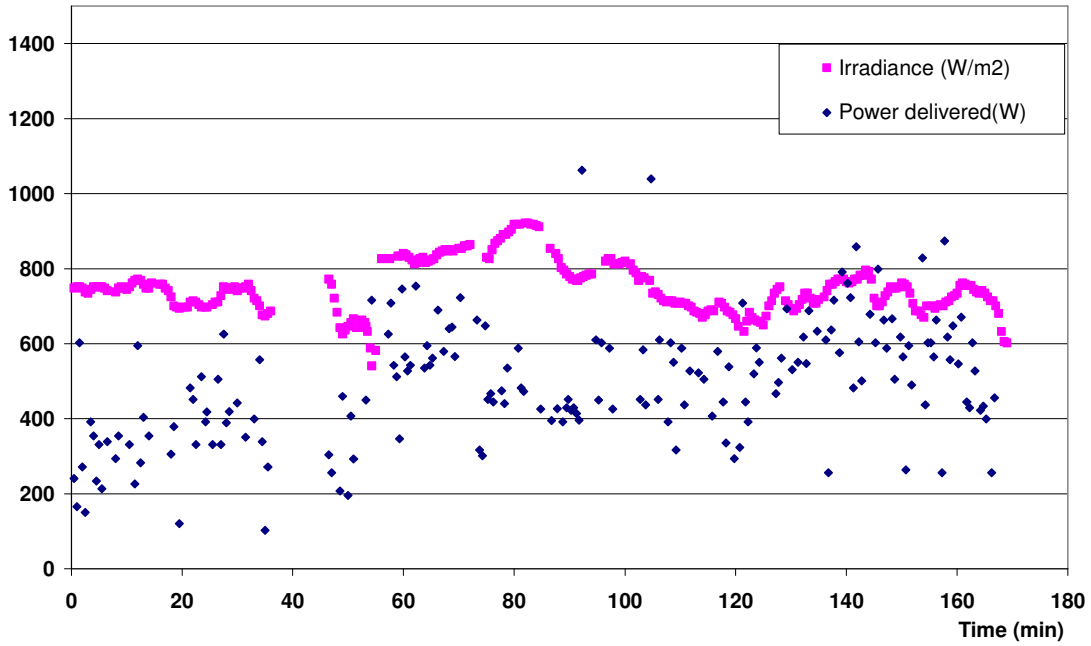

Figure 3.13: Performance of prototype 3: Measured solar irradiance (W/m^2) and produced steam (W) as a function of time. T_0 =18 ^oC.

In the graph it can be seen that the measurements of the steam production are heavily influenced by the wind. The efficiency that was measured was 46%. The efficiencies were calculated as a function of time. The values are depicted in figure 3.14.

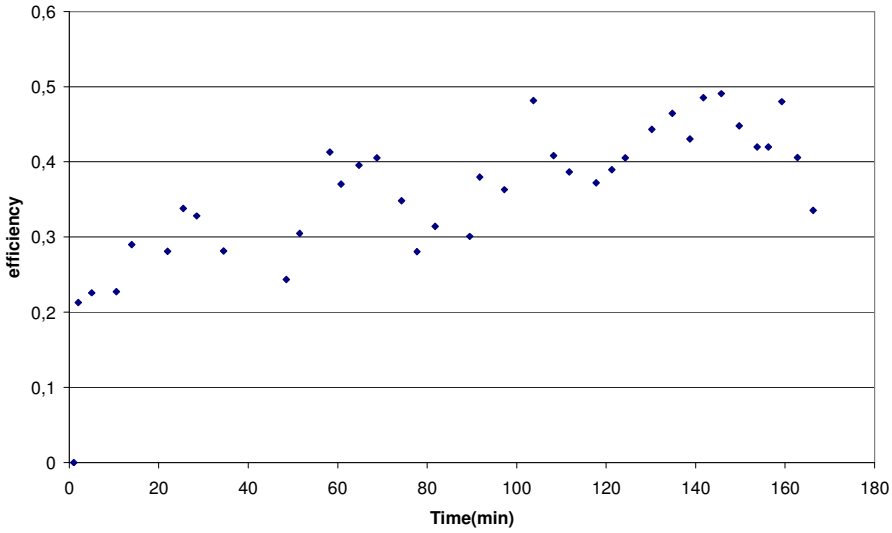

Figure 3.14: Efficiencies as a function of time for prototype 3

These efficiency values are comparable to the typical efficiencies obtained using evacuated tube collectors. The model predicts an efficiency of 56%. The experimental efficiency can be higher if more care is taken to prevent fouling of the selective surface during construction of the boiler and when the solar influx is higher. Furthermore the weighed condensed steam was captured in an open vessel. This setup gives rise to evaporation of the condensate. This leads to lower readings.
The measurements were taken on 18 October 2005. This was the last sunny day of 2005. The ten-year average insolation of Amsterdam is depicted in figure 3.15.

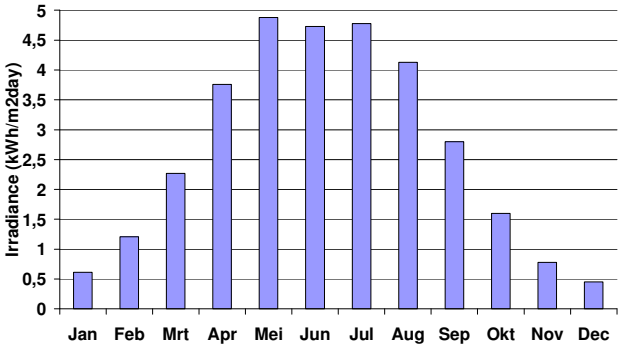

Figure 3.15: Ten-year average solar insolation for Amsterdam (ref 1).

From this graph it becomes apparent that it is difficult to do measurements between October and March.

The boiler was fitted with a clean selective surface and tested next spring, First the boiler was heated up using the reflectors. After the initial heat up the reflectors were taken away after 20 minutes of measuring.(fig 3.16)

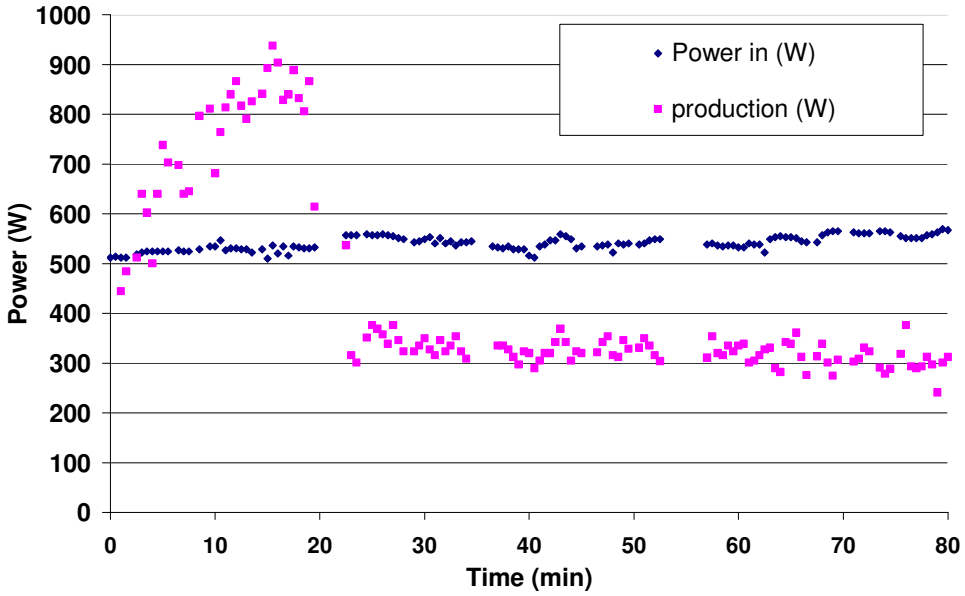

Figure 3.16: Steam produced as a function of time for prototype 3. $T_0=7^0C$

The illuminated area is 0.6m^2. The power that was delivered is 335 W. The efficiency is 61%. The model predicts an efficiency of 62% using a hemispherical absorption coefficient of 96.1%. Thus it can be concluded that model is able to predict the performance of the boiler very well. Furthermore it can be concluded that the hemispherical absorption coefficient of the coating is very close to the normal property. The efficiency of this boiler is greater than the efficiency of evacuated collectors currently on the market. There are two effects that may cause overestimation of the efficiency. The first effect is condensation in the pyranometer. The cold weather caused condensation of water in the pyranometer. However the effect seems small because an irradiance of between 500 w and 600 w was measured as can be seen in the graph. This equates to 833-1000W/m^2.
The other effect is caused by the covering of the reflectors. The reflectors were covered with plates of hardboard on the bottom and blue woven plastic sheet for the back reflector. The dark blue plastic sheet has some light reflecting from it. The hardboard plates do not have any light reflecting from it. Irrespective of both these minor effects a steam production of 558 W/m^2 at a temperature difference of 93^{o}C is considered a very good result.

4. Future work

The results from the research show that the rotating solar boiler may contribute to sustainable energy production. However many aspects of the rotating solar boiler could not be investigated due to a lack of time. Therefore some suggestions for future work are given in this chapter.

4.1 The Inflatable solar boiler

The economic analysis showed that the boiler should be lightweight in order to reduce the pay back time. There are possibilities to reduce the weight of the boiler. Prototype 3 has a very light absorber and cover tube (6.8 kg/m^2). The weight per absorber area is much smaller than that of other collectors. However if the size of the boiler is expanded the structure may become fragile.
In order to reduce the weight and keep a sturdy structure an inflatable rotating solar boiler is proposed. The current boiler already has an inflatable cover and this design can be expanded to also include an inflatable absorber. Inflatables can be very sturdy and light. Examples of this are boats, tires and hovercrafts.
Inflatable roof lights are another example of durable transparent inflatables that can be used outdoor on a permanent basis as can be seen in figure 4.1:

Figure 4.1: Inflated roof lights produced by Buitink technology

An inflatable absorber was used for some experimentation as can be seen in figures 4.2 and 4.3.

Figure 4.2: Deflated boiler

Figure 4.3: Rotating boiler with inflated absorber and cover

The pictures clearly show that a slight overpressure (<100 Pa) in the absorber yields a very stiff structure that can support itself over 3 meters. The absorber is made from flexible aluminum duct. These ducts are very light, cheap and are able to resist the operating temperatures. Furthermore aluminum is a very good substrate for selective coatings. This absorber tube costs only 24€ (excl. BTW) and has a diameter of 0.4m and a length of 3m. This absorber thus costs 20€/m^2. The absorber for prototype 2 costs 61.58 €/m^2 and the absorber for prototype 3 costs 54.1€/m^2. It should be noted that the investigated boilers can already be cheaper than flat plate collectors. An inflatable boiler can reduce the pay back time for the material cost to less than one year.
In the inflatable design the pressure in the absorber is larger than the pressure in the cover. If the absorber is not completely steam proof condense will form on the cover as can be seen in figure 4.4

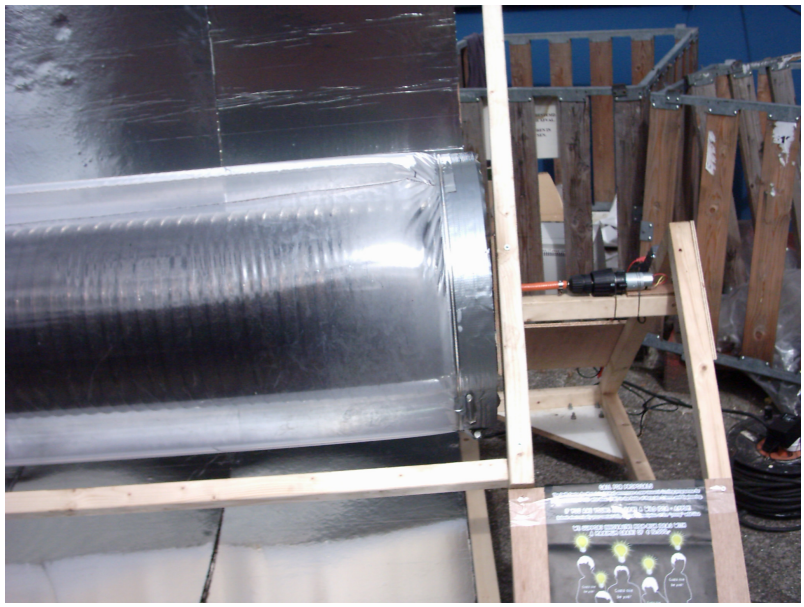

Figure 4.4: Leaks in the absorber lead to condensation on the inside of the cover due to the higher absorber pressure

The flexible aluminum tube is very prone to fatigue cracking and punctures. Therefore it should be handled very carefully and should preferably be inflated only once. Because the heavier steel and copper tubes can also be economically feasible the focus of the research was put on proving the principle of the rotating solar boiler.
Making inflatable rotating solar boilers is deemed a very attractive option because of the size advantage inflatables have. If the boiler is bigger, less relative costs for the sides, the motor, the control system, the seals, the pumps and the frame are expected. Therefore, the inflatable solar boiler should be included in future work. The cost reduction may make the tubes cheaper than the mirrors. This will make the mirrors redundant.

4.2 System control

In order to make a rotating solar collector that can operate unattended, control systems are needed. A distinction must be made between a commercial rotating solar collector and the experimental solar collector. The experimental solar collector requires sensors to determine the efficiency. The most basic commercial solar collector only needs a means of controlling the water load. The efficiency is determined by comparing the heat flow with the power supplied by a pyranometer. The only actuator in the system is a valve or pump to supply water to the collector. This actuator should react to a low water load.
The mass of water present in the system is important. If too much water is present the collector becomes too heavy and if there is too little water or the water is not distributed well overheating may take place. The mass of water gradually decreases due to the evaporation. Therefore new water needs to enter the absorber to maintain the correct load of water. It is important to measure if there is still enough water present. This data is used to control the water inlet valve or pump.

Nine methods were conceived that can do the trick:

1. Manual
   The prototype was filled manually. When it appeared that the steam production decreased, more water was added. Shaking the boiler could indicate if water was present. This operation may have some benefits for experimental purposes but is not considered further.

2. Weighing
   Weighing may be done continuously or each day. It is possible to load all the water for one day into the collector.
   The disadvantage of reloading each day is that it is labor intensive. Continuous weighing is less labor intensive than manual. Another advantage is that the data concerning the water load are obtained in the stationary part of the collector
   Complicating factors for weighing continuously are vibration, and a more complex construction. Weighing also has a disadvantage if salts build up in the absorber.

3. Water sensors
   A water sensor consists of two electrodes that make contact on emersion in impure water. The ions conduct electricity, making the resistance of the sensor less than infinite. The electrodes must resist corrosion. This is considered an important option, because it is easy to incorporate more than two electrodes. A drawback is that the absorber rotates, complicating data transmission (see also paragraph 4.2.1).

4. Temperature sensors
   A temperature sensor was present in prototype 1. If no water is present in the absorber, the temperature will increase beyond 100 ^{o}C. This method is easier than water sensors, because no corrosion issues come into play. Therefore this method may prove to be more reliable in the long run because corrosion can be prevented. However data transmission problems are the same as with water sensors. Another drawback may be that the temperature only increases after all the water has gone. Efficiency may have decreased long before all the water has gone.

5. Heat up/cool down mass determination
   If the collector does not work in steady state, the thermal mass in the absorber determines the heat up or cool down speed. So if there is more water in the absorber it will heat up and cool down slower. Because the sun shines only during the day, heat up and cool down will occur. In order to measure thermal mass, the solar irradiance and absorber temperature should be determined. Drawback of this method is that no measurements can be done if the absorber is in steady state. This method was therefore discarded.

6. Mass inflow and outflow determination
   It is possible to calculate the water mass present in the boiler by measuring the inflow and outflow of mass. A disadvantage is that a steam flow meter is required on commercial collectors. Also any errors in the measurement will propagate in time. This option was used during the experiments, but should not be used in commercial collectors.

7. Motor operation analysis
   If the absorber has a bigger mass, the motor requires more energy to accelerate it. Because the theory suggest a rotation speed exists where no convection occurs at all, it may be possible to accelerate and decelerate above that speed without affecting the efficiency of the boiler. The power consumption of the motor during acceleration/deceleration provides an estimate for the mass of the collector. Wind may affect this kind of measurement, but a great advantage is that only passive electronic components are needed. No sensors, power supplies or brushes are needed.

8. Overflow
   An overflow could also prevent too high water loads. If there is too much water in the absorber it may flow out. This method would make it possible to clean the absorber from residues in the water. It also is possible to generate the heat at lower temperatures by adding more water. Because the boiler is rotating a design for an overflow is not straightforward. Overflows in non-rotating equipment rely on gravity.
   In the water layer of the rotating boiler the centrifugal force is greater than the gravitational force. An overflow can depend on either one of these forces.

9. Heat pipe
   Heat pipes are heat-transferring systems that are closed and have a heat transfer fluid in them. The solar boiler can act as heat pipe where water evaporates in the absorber, condenses in an external heat exchanger and then flows back into the absorber. Because the system is closed the weight of the water (or other heat transfer fluid) is constant. Evacuated tube collectors are often fitted with heat pipes.
   The pressure inside a heat pipe is dependent on the temperature. Because the absorber should be very thin, no pressure fluctuations can be tolerated. An atmospheric heat pipe may be used. Such a heat pipe can only deliver the heat at the boiling point of the heat transfer fluid.

4.2.1 Data transmission

If the amount of water is determined in the absorber (water or temperature sensor), a connection to the control system is required. This is not straightforward because the absorber rotates. The data may be transferred using brushes, or remote control. Prototype 1 used brushes to connect an NTC-temperature sensor to a multimeter. It was observed

that the improvised brushes gave rise to considerable noise in the signal. This is because the brushes do not make contact all the time and the resistance of this setup fluctuated (figure 4.5)

Figure 4.5: Brushes enable temperature measurement inside prototype 1.

Therefore, another data transmission system can better be used. A viable option for data transmission is to use brushes that transmit a frequency instead of a current. The frequency should be a function of the water load. This approach can give much more accurate readings of the water load because the brushes cannot alter the frequency.

4.2.2 Choice of water loading determination

After the preliminary evaluation of the conceived methods for sensing water mass, the viable remaining choices are listed in table 4.1:

Table 4.1: Comparison of various sensing methods

Sensing method	*Data transmission necessary*	*Cause of deviation*
Weighing	No	Salt distribution/ water maldistribution
Water sensors	Yes	-
Temperature sensors	Yes	-
Mass in/outflow determination	No	Time
Motor operation analysis	No	Wind/salt deposition
Overflow	No	-
Heat pipe	No	-

It can be concluded that there are sufficient opportunities to determine the water load in the boiler.

5. List of symbols

a	Heat diffusion coefficient	$[m^2s^{-1}]$
A	Area	$[m^2]$
Cp	Heat capacity	$[JKg^{-1}K^{-1}]$
d	Thickness of the layer	[m]
g	The gravitational constant	$[ms^{-2}]$
Gr	Grashof number	[-]
l	Length of the tube	[m]
m	Number of mirrors/concentration factor	[-]
Nu	Nusselt number	[-]
Pr	Prandtl number	[-]
R	Radius	[m]
r	Reflectivity of the mirrors	[-]
T	temperature	[K]
v	Velocity	[m/s]

Greek symbols

α	Absorption coefficient	[-]
δ_i	Angle of incidence	$[^o]$
Δ	Difference	[-]
ε	Emission coefficient	[-]
η	Efficiency	[-]
Φ	Heat flow	[W]
Φ''	Heat flux	$[W/m^2]$
λ	Heat transfer coefficient	[W/mK]
ν	Kinematic viscosity	$[m^2s^{-1}]$
ρ	Density	$[kgm^{-3}]$
τ	Transmission coefficient	[-]
σ	Stefan-Boltzmann constant	$[Wm^{-2}K^{-4}]$

Subscripts

a	Absorber
c	Cover
e	End caps
h	Hemispherical
i	Illuminated
n	Normal
o	Optical
s	Solar

Superscripts

$cond$	Conductive
$conv$	Convective
in	Incoming
max	Maximum
rad	Radiative

6. Words of appreciation

Many wonderful people helped me to make this research what it is.
First of all I would like to thank my graduation committee Prof. Dr. G.J. Witkamp, Ir. A. Schmets and Drs. J. van Spronsen. I would also like to thank the people from the Delft centre of materials and particularly Dr. S. Luding for their financial support and the people from the workshop of the Laboratory for Process Equipment for their practical support: Jos, Stefan, Gerard, Martijn, Jan and André.
I owe much to the good people from Alanod Sunselect and Inventum for their contributions of selective materials.
I would like to thank my family and my girlfriend Maaike for their continuous support throughout my study.

7. References

1. Apricus, Solar Technology, http://www.apricus-solar.com/insolation_levels_europe.htm, found November 2005
2. Intergas, price of natural gas in the Netherlands for domestic consumption, http://www.intergas.nl/, found August 2005
3. W. Weiss, *Solar Heat for Industrial Processes*, International Energy Agency, Austria, **2003**
4. J. Burch, J. Salasovich, T. Hillman, *Cold-Climate Solar Domestic Water Heating Systems: Life-Cycle Analyses and Opportunities for Cost Reduction,* Proceedings of ISES Solar World Conference, Orlando, **2005**
5. Mök Industries, Concentrating Solar Collector, http://www.mokindustries.com/images/solar-panel1.jpg, found October 2005
6. Renewable Energies, Flat Plate Solar Collector, http://nesa1.uni-siegen.de/wwwextern/idea/keytopic/2.htm, found October 2005
7. Ritter Solar Energy, Evacuated Tube Solar Collector, http://www.solarenergyirelland.com, found October 2005
8. Solar Hot Water Center, Reflectors for Evacuated Tube Solar Collectors, http://www.linuo.co.nz/solar.html, found October 2005
9. Hot sun industries, picture of an uncovered absorber www.powermat.com, found September 2005
10. Research institute for renewable energy, schematics of a solar pond http://reslab.com.au/resfiles/lowtemp/text.html, Found August 2005
11. H.E.A. van den Akker, R.F. Mudde, *Fysische transportverschijnselen 1,* **1998,**142
12. A. F. Mills, *Basic Heat and Mass Transfer*, Prentice Hall, **1999**, 487
13. Q. C. Zhang, D. R. Mills, High Solar Performance Selective Surface Using Bi-Sublayer Cermet Film Structures, *Solar Energy Mater. & Solar Cells* **1992**, 27(3), 273-290
14. T. Tesfamichael, *Characterization of Selective Solar Absorbers*, Acta Universitatis Upsaliensis, Uppsala, **2000**, 57
15. N. C. Bhowmik, J. Rahman, M. A. Alam Khan, Z. H. Mazumder, Preparation of Selective Surfaces and Determination of Optimum Thickness for Maximum Selectivity, *Renewable Energy* **2001**, 24(4), 663-666
16. S. Süzer, F. Kadirgan, H. M. Söhmen, XPS Characterization of Co and Cr Pigmented Copper Solar Absorbers, *Solar Energy Mater. & Solar Cells* **1999**, 56(2), 183-189
17. M. F. Shaffei, S. S. Abd El-Rehim, N. A. Shaaban, H. S. Huisen, Electrolytic Coloring of Anodic Aluminum for Selective Solar Absorbing Films: Use of Additives Promoting Color Depth and Rate, *Renewable Energy* **2001**, 23(3), 489-495
18. Y. Cao, X. Hu, Absorbing Film on Metal for Solar Selective Surface, *Thin Solid Films* **2000**, 375(1), 155-158
19. T. Möller, D. Hönicke, Solar Selective Properties of Electrodeposited Thin Layers on Aluminium, *Solar Energy Mater. & Solar Cells* **1998**, 54(4), 397-403

20. C. Nunes, V. Teixeira, M. Collares-Pereira, A. Monteiro, E. Roman, J. M. Gago, Deposition of PVD Solar Absorber Coatings for High-Efficiency Thermal Collectors, *Vacuum* **2002**, 67(4), 623-627
21. E. Wäckelgård, Characterization of Black Nickel Solar Absorber Coatings Electroplated in a Nickel Chlorine Aqueous Solution, *Solar Energy Mater. & Solar Cells* **1998**, 56(1), 35-44
22. V. Teixeira, E. Sousa, M. F. Costa, C. Nunes, L. Rosa, M. J. Carvalho, M. Collares-Pereira, E. Roman, J. Gago, Chromium-Based Thin Sputtered Composite Coatings for Solar Thermal Collectors, *Vacuum* **2002**, 64(3), 299-305
23. Z. C. Orel, M. K. Gunde, A. Lenček, N. Benz, The Preparation and Testing of Spectrally Selective Paints on Different Substrates for Solar Absorbers, *Solar Energy* **2000**, 69(Suppl.), 131-135
24. M. K. Alam Khan, Copper Oxide Coatings for Use in Linear Solar Fresnel Reflecting Concentrating Collector, *Renewable Energy* **1999**, 17(4), 603-608
25. L. Arurault, J. Salmi, R. S. Bes, Comparison of AC Voltage and Periodic-Reverse Current Nickel Pigmented Anodized Aluminium as Solar Selective Absorber, *Solar Energy Mater. & Solar Cells* **2004**, 82(3), 447-455
26. A. Wazwaz, J. Salmi, H. Hallak, R. Bes, Solar Thermal Performance of a Nickel-Pigmented Aluminium Oxide Selective Absorber, *Renewable Energy* **2002**, 27(2), 277-292
27. S. Süzer, F. Kadirgan, H. M. Söhmen, A. J. Wetherilt, İ. E. Türe, Spectroscopic Characterization of Al_2O_3-Ni Selective Absorbers for Solar Collectors, *Solar Energy Mater. & Solar Cells* **1998**, 52(1), 55-60
28. F. Kadirgan, M. Söhmen, İ. E. Türe, S. Süzer, J. Wetherilt, A. Yazar, An Investigation on the Optimization of Electrochemically Pigmented Aluminium Oxide Selective Collector Coatings, *Renewable Energy* **1997**, 10(2), 203-206
29. L. Kaluža, B. Orel, G. Dražič, M. Kohl, Sol-Gel Derived $CuCoMnO_x$ Spinel Coatings for Solar Absorbers: Structural and Optical Properties, *Solar Energy Mater. & Solar Cells* **2001**, 70(2), 187-201
30. P. Konttinen, P. D. Lund, R. J. Kilpi, Mechanically Manufactured Selective Solar Absorber Surfaces, *Solar Energy Mater. & Solar Cells* **2003**, 79(3), 273-283
31. H. Sai, H. Yugami, Y. Kanamori, K. Hane, Solar Selective Absorbers Based on Two-Dimensional W Surface Gratings with Submicron Periods for High-Temperature Photothermal Conversion, *Solar Energy Mater. & Solar Cells* **2003**, 79(1), 35-49
32. T. Boström, E. Wäckelgård, G. Westin, Solution-Chemical Derived Nickel-Alumina Coatings for Thermal Solar Absorbers, *Solar Energy* **2003**, 74(6), 497-503
33. Y. Yin, D. R. McKenzie, W. D. McFall, Cathodic Arc Deposition of Solar Thermal Selective Surfaces, *Solar Energy Mater. & Solar Cells* **1996**, 44(1), 69-78
34. N. C. Mehra, S. K. Sharma, Black Nickel-Cobalt: Selective Coatings Prepared by a Conversion Process, *Thin Solid Films* **1988**, 156(1), 93-104
35. A. G. Avila, E. C. Barrera, L. A. Huerta, S. Muhl, Cobalt Oxide Films for Solar Selective Surfaces Obtained by Spray Pyrolisis, *Solar Energy Mater. & Solar Cells* **2004**, 82(2), 269-278

36. L. Aries, D. Fraysse, J. P. Traverse, Growth of Selective Coatings on Stainless Steel, *Thin Solid Films* **1987**, 151(3), 413-428
37. C. E. Kennedy, *Review of Mid- to High- Temperature Solar Selective Absorber Materials*, National Renewable Energy Laboratory, Golden, **2002**
38. Fresnel Formulas, Reflection and Refraction of Light, http://physics.nad.ru/Physics/English/rays_txt.htm, found December 2005
39. L. P. B. M. Janssen, M. M. C. G. Warmoeskerken, *Transport Phenomena Data Companion*, Delft University Press, **1997**, 124
40. R. H. Perry, D. W. Green, *Perry's Chemical Engineering Handbook*, McGraw-Hill, **1999**, 5-28
41. S. P. Chow, G. L. Harding, Angular Dependence of Optical Efficiency of Evacuated Tubular Collectors with Anti-Reflection Coatings and Stationary Specular Reflectors, *Solar Energy* **1985**, 34(6), 489-496
42. J. Muschaweck, W. Spirkl, A. Timinger, N. Benz, M. Dörfler, M. Gut, E. Kose, Optimized Reflectors for Non-Tracking Solar Collectors with Tubular Absorbers, *Solar Energy* **2000**, 68(2), 151-159
43. R. Winston, J. J. O'Gallagher, J. Muschaweck, A. R. Mahoney, V. Dudley, Comparison of Predicted and Measured Performance of an Integrated Compound Parabolic Concentrator (ICPC), *Proc. ASES Annual Conf.*, Washington, **1997**, 41-44
44. Index of refraction of borosilicate glass http://www.valleydesign.com/pr16.htm#7740, found November 2005
45. W.D. Callister, *Materials Science and Engineering; An Introduction*, Wiley, **2003**
46. European Solar Engineering, Cost Calculator for Copper Absorber, weight of flat plate collector and thickness of glass plate, http://www.ese-solar.com, found December 2005

8. List of Appendices

1. Preliminary patent investigation
2. Ray-tracer Qbasic program